MAGIC-TDAS 00-11
000727/W.Wittek

Rotation of the sky image in a camera of telescopes with ALT-AZ mount

W. Wittek
(Max-Planck-Institut fuer Physik, Munich)

27th July, 2000

Abstract

With an earth-based telescope with ALT-AZ mount the sky image in the camera rotates when a source is tracked. The formulas for the rotation angle and the rotation speed as well as for the rotations of the telescope are given as a function of the zenith and azimuthal angle, and as a function of declination and hour angle. The special case of a telescope at La Palma is discussed.

1 Introduction

One of the advantages of telescopes with an equatorial mount is the fact that the sky image in the camera does not change when a source is tracked. This is not the case for earth-based telescopes which have an ALT-AZ mount and which are not located at the north or the south pole. In this case the sky image rotates.

In particular, bright stars in the field of view of the telescope will move on circular lines in the camera during tracking of a source. These steadily changing background conditions have to be taken into account in the data taking, in the trigger and in the offline analysis. Data providing information on the pedestals and their fluctuations have to be taken more frequently than in the case without such a rotation. This is necessary because the fluctuations of the pedestal for a particular pixel of the camera will change drastically when a star image is moving over the pixel.

The rotation may be compensated by rotating the camera during tracking. The negative features of such a design (larger size and weight of the camera, etc.) are not discussed here.

In this report the formulas for the rotation angle and the rotation speed as well as for the rotations of the telescope are derived as a function of the zenith and azimuthal angle and as a function of the declination and the hour angle. The particular example of a telescope at La Palma is discussed.

2 Coordinate systems

Local coordinate systems (A), with the 3rd axis pointing into the direction opposite to the zenith (see Fig. 1)

$$\vec{r}_{\mathrm{A}} = \begin{pmatrix} x_{\mathrm{A}} \\ y_{\mathrm{A}} \\ z_{\mathrm{A}} \end{pmatrix} = \begin{pmatrix} \sin\theta \, \cos\varphi \\ \sin\theta \, \sin\varphi \\ -\cos\theta \end{pmatrix} \tag{1}$$

θ zenith angle
φ azimuthal angle ($\varphi = 0$ in north direction, φ increasing from north to east, south, west, north)

The angles θ ($= 90° -$ ALT) and φ ($=$ AZ) are a natural choice of angles for a telescope with ALT-AZ mount (see Fig. 2).
Equatorial coordinate system (B), with the 3rd axis being antiparallel to the rotation axis of the earth (see Fig 1).

$$\vec{r}_{\mathrm{B}} = \begin{pmatrix} x_{\mathrm{B}} \\ y_{\mathrm{B}} \\ z_{\mathrm{B}} \end{pmatrix} = \begin{pmatrix} \cos\delta \, \cos\phi \\ \cos\delta \, \sin\phi \\ -\sin\delta \end{pmatrix} \tag{2}$$

δ declination
ϕ hour angle ($\phi = 0$ when source is culminating at the geographical longitude of the telescope)

The angles δ and ϕ are very convenient for describing the trajectories of sources, because for a given source $\delta = \delta_{\mathrm{source}} =$ constant and ϕ increases at the constant rate $d\phi/dt = \dot{\phi} =$ (360° per sideric day) $= 360°/(0.9972696 \times 24\ \mathrm{h})$ (see Fig. 2).
The definition of the angles agrees with the most commonly used definition. The direction of the axes of the two cartesian coordinate systems was chosen such that the usual relation between the angles and the x, y coordinates is preserved, and that both systems are right-handed.
The transformation of the representation $\vec{r}_{\mathrm{A}}$ of a vector $\vec{r}$ in system A into the representation $\vec{r}_{\mathrm{B}}$ in system B and vice versa is given by

$$\vec{r}_{\mathrm{B}} = A\,\vec{r}_{\mathrm{A}} \qquad \vec{r}_{\mathrm{A}} = A\,\vec{r}_{\mathrm{B}} \tag{3}$$

with

$$A = \begin{pmatrix} +a_3 & 0 & -a_1 \\ 0 & -1 & 0 \\ -a_1 & 0 & -a_3 \end{pmatrix} \tag{4}$$

Here $a_1 = \cos(\mathrm{Lat})$ and $a_3 = -\sin(\mathrm{Lat})$, where Lat is the geographical latitude of the observing telescope (see Sect. 5). The transformation A is an orthogonal transformation with $A = A^{\mathrm{T}} = A^{-1}$ and $\det(\mathrm{A}) = 1$.

The representations of the zenith direction $\vec{z}$ and of the earth-rotation axis $\vec{a}$ (pointing to the celestial north pole) in the two systems are:

	system A	system B
$\vec{z}$	$(0,\ 0,\ -1)$	$(a_1,\ 0,\ a_3)$
$\vec{a}$	$(a_1,\ 0,\ a_3)$	$(0,\ 0,\ -1)$

(5)

Equations (1), (2), (3) and (4) give the relations between (θ, φ), and (δ, ϕ)

$$\begin{aligned} \cos\delta\cos\phi &= \quad a_3\sin\theta\cos\varphi + a_1\cos\theta \\ \cos\delta\sin\phi &= \quad -\sin\theta\sin\varphi \\ -\sin\delta &= -a_1\sin\theta\cos\varphi + a_3\cos\theta \end{aligned} \tag{6}$$

$$\begin{aligned} \sin\theta\cos\varphi &= \quad a_3\cos\delta\cos\phi + a_1\sin\delta \\ \sin\theta\sin\varphi &= \quad -\cos\delta\sin\phi \\ -\cos\theta &= -a_1\cos\delta\cos\phi + a_3\sin\delta \end{aligned} \tag{7}$$

These relations are shown in Figs. 3 and 4 for a telescope at La Palma (Lat $= 28.8°$, see section 5). In Fig. 3 the lines of constant δ and ϕ are drawn in the $(\cos\theta, \varphi)$ plane. The lines of constant δ correspond to the trajectories of sources. One can see that for $\delta > \mathrm{Lat}$ and $\delta < -\mathrm{Lat}$ the range of φ is restricted, whereas for $-\mathrm{Lat} < \delta < \mathrm{Lat}$ the full range of φ is covered. Of course, the points below the horizon ($\cos\theta < 0$) are not observable.

In Fig. 4 the lines of constant θ and φ are drawn in the $(\sin\delta, \phi)$ plane. The plot shows how for a given source, i.e. for a fixed δ, a restriction in the zenith angle θ is transformed into a restriction of the hour angle ϕ (see also Fig. 19). This is discussed in more detail in Sect. 7.

If $\widetilde{\varphi} = \varphi - 180°$ is used instead of φ, then $\sin\varphi$ has to be replaced by $-\sin\widetilde{\varphi}$ and $\cos\varphi$ by $-\cos\widetilde{\varphi}$, in the formulas (1), (6) and (7). The representations (5) and the expression (4) for A, with $a_1 = \cos(\mathrm{Lat})$ and $a_3 = -\sin(\mathrm{Lat})$, remain unchanged, because the redefinition of the zero-point of φ affects only the relation between $(x_{\mathrm{A}}, y_{\mathrm{A}})$ and (θ, φ), but not the definition of the coordinate system A.

If the altitude ALT $= 90° - \theta$ is used instead of the zenith angle θ, then in the formulas (1), (6) and (7) $\sin\theta$ has to be replaced by cos(ALT), and $\cos\theta$ by sin(ALT).

3 General expressions for the rotation angle and the rotation speed of the sky image in the camera

a) Rotation angle

The rotation angle α is calculated as the angle between a reference direction $\vec{e}_{\mathrm{c}}$ in the camera and a reference direction $\vec{e}_{\mathrm{s}}$ in a local sky region (see Fig. 5). If $\vec{r}$ denotes the position of the source (= direction in which the telescope is pointing) the two reference directions may be defined as

$$\vec{e}_{\mathrm{c}} = \frac{\vec{r} \times \vec{z}}{|\vec{r} \times \vec{z}|} \qquad \vec{e}_{\mathrm{s}} = \frac{\vec{r} \times \vec{a}}{|\vec{r} \times \vec{a}|} \tag{8}$$

$\vec{r}$ specifies a point on the surface of a sphere with its center at the telescope (see Fig. 2). $\vec{e}_{\mathrm{c}}$ is the tangent vector at this point to the circle $\theta =$ constant, and $\vec{e}_{\mathrm{s}}$ is the tangent vector at this point to the circle $\delta =$ constant on the sphere.

α is then obtained from

$$\cos\alpha = \vec{e}_{\mathrm{s}} \cdot \vec{e}_{\mathrm{c}} \tag{9}$$

$$\sin\alpha = (\vec{e}_{\mathrm{c}} \times \vec{r}) \cdot \vec{e}_{\mathrm{s}} = -(\vec{e}_{\mathrm{c}} \times \vec{e}_{\mathrm{s}}) \cdot \vec{r} \tag{10}$$

$$= \frac{-(\vec{r} \times \vec{z}) \cdot \vec{a}}{|\vec{r} \times \vec{z}|\,|\vec{r} \times \vec{a}|}$$

b) Rotation speed

When a source is tracked with the telescope one moves along the line $\delta = \delta_{\mathrm{source}}$, while ϕ is increasing at a rate

$$\frac{d\phi}{dt} = \dot{\phi} = \frac{360°}{0.9972696 \times 24\ \mathrm{h}} \tag{11}$$

The rotation speed $d\alpha/dt$ of the sky image in the camera during tracking can therefore be determined as

$$\frac{d\alpha}{dt} = \frac{d\alpha}{d\phi} \cdot \frac{d\phi}{dt} = \alpha' \cdot \dot{\phi} \tag{12}$$

For calculating α' the following relations are useful:

$$\begin{aligned}
\frac{d\alpha}{d\cos\alpha} &= -\frac{1}{\sin\alpha} && = \frac{1}{(\vec{e}_c \times \vec{e}_s)\cdot\vec{r}} \\
\frac{d\vec{r}}{d\phi} &= \vec{r}\,' && = \vec{r}\times\vec{a} \\
\frac{d\vec{e}_s}{d\phi} &= \vec{e}_s\,' && = \vec{e}_s\times\vec{a} \\
\frac{d\vec{e}_c}{d\phi} &= \vec{e}_c\,' && = \frac{|\vec{r}\times\vec{a}|}{|\vec{r}\times\vec{z}|}\Big\{(\vec{e}_s\times\vec{z}) - \vec{e}_c[(\vec{e}_c\times\vec{e}_s)\cdot\vec{z}]\Big\} \\
\vec{e}_c\times\vec{e}_s &= \frac{(\vec{r}\times\vec{z})\cdot\vec{a}}{|\vec{r}\times\vec{z}|\,|\vec{r}\times\vec{a}|}\,\vec{r}
\end{aligned}$$

$$\begin{aligned}
\frac{d\cos\alpha}{d\phi} &= \vec{e}_s\,'\cdot\vec{e}_c + \vec{e}_s\cdot\vec{e}_c\,' \\
&= (\vec{e}_c\times\vec{e}_s)\cdot\vec{a} - \frac{|\vec{r}\times\vec{a}|}{|\vec{r}\times\vec{z}|}\,(\vec{e}_s\cdot\vec{e}_c)\,[(\vec{e}_c\times\vec{e}_s)\cdot\vec{z}]
\end{aligned}$$

For α' one obtains

$$\begin{aligned}
\alpha' = \frac{d\alpha}{d\phi} &= \frac{d\alpha}{d\cos\alpha}\cdot\frac{d\cos\alpha}{d\phi} \\
&= \left\{(\vec{e}_c\times\vec{e}_s)\cdot\vec{a} - \frac{|\vec{r}\times\vec{a}|}{|\vec{r}\times\vec{z}|}(\vec{e}_s\cdot\vec{e}_c)[(\vec{e}_c\times\vec{e}_s)\cdot\vec{z}]\right\}\cdot\frac{1}{(\vec{e}_c\times\vec{e}_s)\cdot\vec{r}} \\
&= (\vec{a}\cdot\vec{r}) - \frac{|\vec{r}\times\vec{a}|}{|\vec{r}\times\vec{z}|}(\vec{e}_s\cdot\vec{e}_c)(\vec{z}\cdot\vec{r}) && (13) \\
&= \frac{(\vec{a}\times\vec{z})\;\cdot\;(\vec{r}\times\vec{z})}{(\vec{r}\times\vec{z})^2} && (14)
\end{aligned}$$

4 Formulas for the rotation angle and the rotation speed of the sky image in the camera

a) The rotation angle as a function of θ and φ, or δ and ϕ.

Evaluating eqs. (8), (9) and (10) yields the rotation angle α as a function of the zenith and azimuthal angles θ and φ, or as a function of the declination and the hour angles δ and ϕ.

$$\cos\alpha \;=\; \vec{e}_s \cdot \vec{e}_c \;=\; \frac{\vec{r}\times\vec{a}}{|\vec{r}\times\vec{a}|} \cdot \frac{\vec{r}\times\vec{z}}{|\vec{r}\times\vec{z}|}$$

$$\begin{aligned}(\vec{r}\times\vec{a})\cdot(\vec{r}\times\vec{z}) &= (\vec{z}\cdot\vec{a})\cdot\vec{r}^{\,2} - (\vec{z}\cdot\vec{r})(\vec{a}\cdot\vec{r}) \\ &= -a_3 - \cos\theta\,(a_1\sin\theta\cos\varphi - a_3\cos\theta) \\ &= -a_3 - \sin\delta\,(a_1\cos\delta\cos\phi - a_3\sin\delta)\end{aligned} \tag{15}$$

$$\begin{aligned}|\vec{r}\times\vec{z}| &= \sin\theta \\ &= \sqrt{(\cos\delta\sin\phi)^2 + (a_1\sin\delta + a_3\cos\delta\cos\phi)^2}\end{aligned} \tag{16}$$

$$\begin{aligned}|\vec{r}\times\vec{a}| &= \sqrt{(\sin\theta\sin\varphi)^2 + (a_1\cos\theta + a_3\sin\theta\cos\varphi)^2} \\ &= \cos\delta\end{aligned} \tag{17}$$

Thus

$$\cos\alpha = \frac{-a_3\sin\theta - a_1\cos\theta\cos\varphi}{\sqrt{(\sin\theta\sin\varphi)^2 + (a_1\cos\theta + a_3\sin\theta\cos\varphi)^2}} \tag{18}$$

$$= \frac{-a_3\cos\delta - a_1\sin\delta\cos\phi}{\sqrt{(\cos\delta\sin\phi)^2 + (a_1\sin\delta + a_3\cos\delta\cos\phi)^2}} \tag{19}$$

and

$$\sin\alpha \;=\; -(\vec{e}_c\times\vec{e}_s)\cdot\vec{r} \;=\; \frac{-(\vec{r}\times\vec{z})\cdot\vec{a}}{|\vec{r}\times\vec{z}||\vec{r}\times\vec{a}|}$$

$$= \frac{+a_1\cdot\sin\varphi}{\sqrt{(\sin\theta\sin\varphi)^2 + (a_1\cos\theta + a_3\sin\theta\cos\varphi)^2}} \tag{20}$$

$$= \frac{-a_1\sin\phi}{\sqrt{(\cos\delta\sin\phi)^2 + (a_1\sin\delta + a_3\cos\delta\cos\phi)^2}} \tag{21}$$

For determining α the calculation of $\cos\alpha$ and of the sign of $\sin\alpha$ is, of course, sufficient.

b) The rotation speed as a function of θ and φ, or δ and ϕ.

The rotation speed is calculated from eqs. (11), (12) and (13), using the representations of the vectors $\vec{a}, \vec{r}$ and $\vec{z}$ in the systems A or B, given in eqs. (1), (2) and (5).

$$\alpha' = \frac{d\alpha}{d\phi} = (a_1 \sin\theta \cos\varphi - a_3 \cos\theta) - \frac{\sqrt{(\sin\theta \sin\varphi)^2 + (a_1 \cos\theta + a_3 \sin\theta \cos\varphi)^2} \cdot \cos\alpha \cdot \cos\theta}{\sin\theta}$$

$$= \frac{a_1 \cos\varphi}{\sin\theta} \tag{22}$$

$$= \sin\delta - \frac{\cos\delta \cdot \cos\alpha \cdot (a_1 \cos\delta \cos\phi - a_3 \sin\delta)}{\sqrt{(\cos\delta \sin\phi)^2 + (a_1 \sin\delta + a_3 \cos\delta \cos\phi)^2}}$$

$$= \frac{a_1(a_1 \sin\delta + a_3 \cos\delta \cos\phi)}{(\cos\delta \sin\phi)^2 + (a_1 \sin\delta + a_3 \cos\delta \cos\phi)^2} \tag{23}$$

5 Discussion of the rotation angle for a telescope at La Palma

The geographical coordinates of La Palma are Long = 17.9° W and Lat = 28.8° N, yielding

$$\begin{aligned} a_1 &= \cos(\mathrm{Lat}) &&= 0.8763 \\ a_3 &= -\sin(\mathrm{Lat}) &&= -0.4818 \end{aligned}$$

a) Rotation angle of the sky image in the camera

In Fig. 6 the rotation angle α is plotted as a function of $\cos\theta$ and φ, and in Fig. 7 as a function of $\sin\delta$ and ϕ. The contour plots show the lines of constant α. For the actual observations only the region $\theta < \theta_{\max}$, with $\theta_{\max} \approx 90°$, and the corresponding region in the (δ, ϕ) plane (the region on the right-hand side of the dashed line in Fig. 7) is relevant. For completeness, however, the whole angular region is shown. The restriction $\theta < \theta_{\max}$ and its implications are discussed in Sect. 7.

The functions in the two Figs. 6 and 7 are closely related, which follows directly from the expressions (18) to (21):

$$\alpha = f(\theta, \varphi) = -f(90^\circ - \delta, \phi) = f(90^\circ - \delta, -\phi)$$

Note that along the lines ($\cos\theta > -a_3, \varphi = 0$) and ($\cos\theta < a_3, \varphi = 180^\circ$) in Fig. 6, and along the lines ($\sin\delta > -a_3, \phi = 0$) and ($\sin\delta < a_3, \phi = 12\,\mathrm{h}$) in Fig. 7, there is no discontinuity in α because $\alpha = 180^\circ$ and $\alpha = -180^\circ$ are identical angles.

b) Rotation speed of the sky image in the camera

The corresponding dependences of the rotation speed are given in Figs. 8 and 9. The contour plots in Figs. 8 and 9 show the lines of constant rotation speed.

The following observations can be made:

- For δ > Lat (e.g. Mkn 501) the sky image rotates always anticlockwise ($d\alpha/dt > 0$), for δ < –Lat always clockwise ($d\alpha/dt < 0$). The full range of rotation angles ($-180^\circ \leq \alpha \leq 180^\circ$) is covered (Figs. 7 and 9).
- For $-$Lat < δ < Lat (e.g. the Crab nebula) the sky image rotates partly clockwise and partly anticlockwise. α lies within the region $-90^\circ < \alpha < 90^\circ$ (Figs. 7 and 9).
- The rotation speed has singularities at $(\delta, \phi) =$ (Lat, 0 h) and ($-$Lat, 12 h), which corresponds to $\theta = 0^\circ$ and 180° respectively (Figs. 8 and 9). The singularities are due to the term $1/|\vec{r} \times \vec{z}|$ in eq. (13).
- At $\varphi = 90^\circ$ and -90° the rotation speed is zero, for all $\theta \neq 0^\circ$ and $\neq 180^\circ$ (Fig. 8). This follows directly from eq. (22).

c) Regions where $|d\alpha/dt|$ is large

The regions with large absolute values of $d\alpha/dt$ are investigated in more detail in Figs. 10 and 11. These figures show $d\alpha/dt$ as a function of θ and φ or δ and ϕ, for $\theta < 5^\circ$ and (Lat – 10°) < δ < (Lat + 10°) respectively. The points where $|d\alpha/dt|$ exceeds 500°/h are not shown. The different contours in the contour plots correspond to fixed values of $d\alpha/dt$.

The time during which $|d\alpha/dt|$ exceeds a certain value when a source is tracked (δ fixed at δ_{source}) can be read off directly from the contour plot in Fig. 11.

For a given source, i.e. for a given declination δ, $|d\alpha/dt|$ is maximum when the source is culminating, i.e. when $\phi = 0^\circ$ or 180°. $d\alpha/dt$ for $\phi = 0^\circ$ is plotted in Fig. 12 as a function of δ.

For a given source and for a given value ω_0 the time interval around culmination can be calculated during which $|d\alpha/dt|$ is greater than ω_0. The result is displayed in Fig. 13 as a function of δ for different values of ω_0.

d) Times for passing a pixel in the MAGIC camera

It is of interest to know the time interval for passing one pixel in the camera when the sky image is rotating. With MAGIC, a fine-resolution pixel at the edge of the central camera zone appears under an angle $\Delta\beta_{\mathrm{f}} = 360°/66 = 5.45°$, as seen from the center of the camera. For a low-resolution pixel at the edge of the outer camera zone the angle is $\Delta\beta_{\mathrm{l}} = 360°/48 = 7.5°$.

Thus, if $|d\alpha/dt| \geq w_0$, the time needed for passing a fine-resolution pixel (at the edge of the central camera zone) will be $\Delta\, t_0 \leq \Delta\beta_{\mathrm{f}}/\omega_0$. The Δt_0 values corresponding to the different ω_0 values are given on the right-hand side of Fig. 13.

In Table 1 the approximate times for passing a fine-resolution or a low-resolution pixel are compiled for the most critical cases.

6 The movements of the telescope

With an ALT-AZ mount both angles θ and φ are varying permanently when a source is tracked. The functions $\theta(t)$ and $\varphi(t)$ can be determined using eqs. (7), which relate (θ, φ) with (δ, ϕ), and eq. (11):

$$\begin{aligned}
\cos\theta &= a_1 \cos\delta\cos\phi - a_3 \sin\delta \\
\frac{d\theta}{dt} &= \frac{d\theta}{d\phi} \cdot \frac{d\phi}{dt} \\
\frac{d\theta}{d\phi} &= \frac{d\theta}{d\cos\theta} \cdot \frac{d\cos\theta}{d\phi} \\
& \qquad \frac{d\theta}{d\cos\theta} = \frac{-1}{\sin\theta} \\
& \qquad \frac{d\cos\theta}{d\phi} = -a_1 \cos\delta \sin\phi
\end{aligned}$$

$$\frac{d\theta}{d\phi} = \frac{a_1 \cos\delta\sin\phi}{\sqrt{(\cos\delta\sin\phi)^2 + (a_1 \sin\delta + a_3 \cos\delta\cos\phi)^2}} \qquad (24)$$

The expression for $d\theta/d\phi$ becomes more transparent when it is rewritten as

$$\frac{d\theta}{d\phi} = -\sin\alpha \cdot \cos\delta \;=\; -a_1 \sin\varphi \;=\; (\vec{e}_{\mathrm{c}} \cdot \vec{a}) = \frac{\vec{a} \cdot (\vec{r} \times \vec{z})}{|\vec{r} \times \vec{z}|} \qquad (25)$$

The corresponding calculation for φ reads :

$$\begin{aligned}
\tan\varphi &= \frac{\sin\varphi}{\cos\varphi} = \frac{-\cos\delta\sin\phi}{a_3\cos\delta\cos\phi + a_1\sin\delta} \\
\frac{d\varphi}{dt} &= \frac{d\varphi}{d\phi}\cdot\frac{d\phi}{dt} \\
\frac{d\varphi}{d\phi} &= \frac{d\varphi}{d\tan\varphi}\cdot\frac{d\tan\varphi}{d\phi} \\
& \frac{d\varphi}{d\tan\varphi} = \frac{1}{1+\tan^2\varphi} \\
& \frac{d\tan\varphi}{d\phi} = \frac{(-a_3\cos\delta - a_1\sin\delta\cos\phi)\,\cos\delta}{(a_3\cos\delta\cos\phi + a_1\sin\delta)^2}
\end{aligned}$$

$$\frac{d\varphi}{d\phi} = \frac{(-a_3\cos\delta - a_1\sin\delta\cos\phi)\,\cos\delta}{(\cos\delta\sin\phi)^2 + (a_3\cos\delta\cos\phi + a_1\sin\delta)^2} \tag{26}$$

With (9), (15), (16) and (18) this can be rewritten as

$$\frac{d\varphi}{d\phi} = \frac{\cos\delta\cdot\cos\alpha}{\sin\theta} = \frac{|\vec{r}\times\vec{a}|}{|\vec{r}\times\vec{z}|}\,(\vec{e}_{\mathrm{c}}\cdot\vec{e}_{\mathrm{s}}) \tag{27}$$

$$= \frac{(\vec{r}\times\vec{a})\;\cdot\;(\vec{r}\times\vec{z})}{(\vec{r}\times\vec{z})^2} \tag{28}$$

From (13) and (27) one obtains the relation

$$\frac{d\alpha}{d\phi} = (\vec{a}\cdot\vec{r}) - \frac{d\varphi}{d\phi}\,(\vec{z}\cdot\vec{r}) \tag{29}$$

From (14) and (28) it follows:

$$\frac{d\varphi}{d\phi} = (\vec{z}\;\cdot\;\vec{a}) - \frac{d\alpha}{d\phi}\,(\vec{z}\;\cdot\;\vec{r}) \tag{30}$$

With (30) and (22) the expression for $d\varphi/d\phi$ in terms of θ and φ becomes

$$\frac{d\varphi}{d\phi} = \left(-a_3 - \frac{a_1\cos\theta\cos\varphi}{\sin\theta}\right) \tag{31}$$

The dependence of $d\theta/dt$ on $(\cos\theta,\varphi)$ and on $(\sin\delta,\phi)$ is displayed in Figs. 14 and 15 respectively. The corresponding plots for $d\varphi/dt$ are given in Figs. 16 and 17.

From (25) it follows that $|d\theta/dt|$ is always less than $\dot{\phi}$ (Figs. 14 und 15). $d\varphi/dt$, on the other hand, has singularities at $(\delta, \phi) = (\mathrm{Lat}, 0)$ and $(-\mathrm{Lat}, 12\,\mathrm{h})$, like $d\alpha/dt$. At the singularities θ is equal to 0° or 180°, and $(\vec{z} \cdot \vec{r})$ is +1 or −1 respectively. According to (30) $d\alpha/dt$ is therefore approximately equal to $-d\varphi/dt$ near $\theta = 0°$, and approximately equal to $d\varphi/dt$ near $\theta = 180°$. This is indeed seen in Figs. 9 and 17. The $(\cos\theta, \varphi)$ or $(\sin\delta, \phi)$ regions with large $|d\alpha/dt|$ and those with large $|d\varphi/dt|$ are therefore nearly identical. For the actual observations, of course, only $\theta < \theta_{\mathrm{max}}$ is relevant.

$d\varphi/dt$ for $\phi = 0°$ is plotted in Fig. 18 as a function of δ. As expected from (29) and (30), there is a great simililarity between $d\alpha/dt$ (Fig. 12) and $d\varphi/dt$ (Fig. 18), especially near $\delta = \mathrm{Lat}$.

7 Minimum and maximum values of angles and rotation speeds for real observations by a telescope in La Palma

7.1 Extreme values of the hour angle ϕ

Usually a source (with $\delta = \delta_{\mathrm{source}}$) is only observable if $\theta < 90°$, i.e. $\cos\theta > 0$. Using the last eq. of (7), this condition can be reformulated as

$$0 < \cos\theta = a_1 \cos\delta \cos\phi - a_3 \sin\delta$$

which implies

$$\cos\phi \quad > \quad \frac{a_3 \sin\delta}{a_1 \cos\delta} \qquad = -\tan(\mathrm{Lat}) \;\cdot\; \tan\delta$$

$$= \frac{-\tan\delta}{\tan(90° - \mathrm{Lat})} = \frac{\tan\delta}{\tan(-90° + \mathrm{Lat})} \tag{32}$$

a) Sources which are not observable

For $\delta_{\mathrm{source}} < (-90° + \mathrm{Lat})$ the expression on the right-hand side of (32) is greater than 1, which means that these sources are not observable in La Palma.

b) Sources which are always observable

For $\delta_{\mathrm{source}} > (90° - \mathrm{Lat})$ the expression on the right-hand side of (32) is less than -1, so that condition (32) is fulfilled. These sources are therefore always observable.

c) Sources which are observable part of the time

For the remaining sources, $(-90^\circ + \text{Lat}) < \delta_{\text{source}} < (90^\circ - \text{Lat})$ eq. (32) defines the minimum and maximum values of ϕ during observation:

$$\phi_{\text{extr}} = \pm \arccos \left[\frac{-\tan\delta}{\tan(90^\circ - \text{Lat})} \right] \tag{33}$$

The extreme values of ϕ resulting from the condition $\theta < 90^\circ$ are displayed in Fig. 19 (upper plot) as a function of δ. The region in the (δ, ϕ) plane which is not accessible is shown shaded. The border lines for the conditions $\theta < 105^\circ$, $\theta < 75^\circ$ and $\theta < 61.2^\circ$ are also drawn in the Figure.

7.2 Extreme values of the azimuthal angle φ

From Fig. 3 one can see that the range in the azimuthal angle φ is very different for different regions of δ:

a) for $\delta >$ Lat the range in φ is a region around $\varphi = 0$ with the extreme values of φ given by the condition $d\varphi/d\phi = 0$. Using (26) the condition $d\varphi/d\phi = 0$ yields $\cos\phi = -(a_3 \cos\delta)/(a_1 \sin\delta)$, or

$$\cos\varphi_{\text{extr}} = \frac{\sqrt{\sin^2\delta - a_3{}^2}}{a_1}$$

The range in φ is thus (see Fig. 19, lower plot)

$$-\varphi_{\text{extr}} < \varphi < \varphi_{\text{extr}} = +\arccos\left(\frac{\sqrt{\sin^2\delta - a_3{}^2}}{a_1}\right) \tag{34}$$

b) for $(-90^\circ + \text{Lat}) < \delta <$ Lat the range in φ is a region around $\varphi = 180^\circ$ with the extreme values of φ given by the condition $\cos\theta = 0$. Using the last equation of (6) the condition $\cos\theta = 0$ implies:

$$\cos\varphi_{\text{extr}} = \frac{\sin\delta}{a_1}$$

The range in φ in this case is

$$\varphi_{\text{extr}} = +\arccos\left(\frac{\sin\delta}{a_1}\right) < \varphi < 360^\circ - \varphi_{\text{extr}} \tag{35}$$

The limits in φ given by (34) and (35) are plotted in Fig. 19 (lower plot) as a function of δ. The shaded region denotes the area which is not accessible due to the restriction $\theta < 90°$. The border lines in φ for the conditions $\theta < 105°$, $\theta < 75°$ and $\theta < 61.2°$ are also drawn in the Figure.

An interesting question is, how a telescope has to be constructed so that for any observable source the observation can be performed without interruption. If for example, during observation of a source, the telescope hits the point $\varphi = \varphi_0$ beyond which the telescope cannot be moved, the telescope would have to be rotated back by 360° in φ before the observation could be continued.

From Fig. 19 (lower plot) one can see that the largest regions in φ are covered by sources with δ slightly above Lat or with δ slightly below Lat. These regions are

$$R^+ : \; -\varphi_{\text{extr}} < \varphi < \varphi_{\text{extr}} = +\arccos(0) = 90°$$

which follows from eq. (34) with $\delta = \text{Lat}$, and

$$R^- : \; \varphi_{\text{extr}} = +\arccos\left(\frac{a_3 \cos\theta_{\max} - a_3}{a_1 \sin\theta_{\max}}\right) < \varphi < 360° - \varphi_{\text{extr}}$$

which follows from a generalization of (35) with $\delta = \text{Lat}$.

The two regions are indicated in Fig. 20 by circular lines labeled as R^+ and R^-. A suitable choice of the range in φ, within which the telescope can be moved, and which avoids interruptions of observations is the following:

Take $\varphi_0 = 90°$ (counted from the north direction in the clockwise direction) and construct the telescope such that it is movable, starting from $\varphi = \varphi_0$, by an angle $\Delta = [360° + \varphi_0 - \varphi_1(\theta_{\max})]$ in the anti-clockwise direction to reach $\varphi = \varphi_1$, beyond which point the telescope cannot be moved. Starting from $\varphi = \varphi_1$, it should be possible to move the telescope back in the clockwise direction by the same angle Δ to reach φ_0, beyond which point the telescope cannot be moved. With $\varphi_0 = 90°$ and $\varphi_1(\theta_{\max}) = 44.23°$, $56.65°$, $65.05°$ and $71.02°$ for $\theta_{\max} = 105°$, $90°$, $75°$ and $61.2°$ respectively, Δ becomes 405.8°, 393.4°, 385.0° and 379.0° respectively.

7.3 Extreme values of $d\varphi/dt$

Using eq. (26), the extreme values of $d\varphi/dt$ can be calculated for fixed δ. The constraint $\theta < \theta_{\max}$ is taken into account by searching the minimum and maximum of $d\varphi/dt$ in the ϕ range given by the condition

$$\cos\theta = a_1 \cos\delta \cos\phi - a_3 \sin\delta > \cos\theta_{\max}$$

which follows from the last equation in (7).

The results are shown in Fig. 21 for $\theta_{\max} = 105°$, $90°$, $75°$ and $61.2°$. For $\delta <$ Lat, $d\varphi/dt$ is always positive and the maximum is reached at $\phi = 0$, for all $\theta_{\max}$ (see Fig. 18). The minimum of $d\varphi/dt$, which depends on $\theta_{\max}$, is in the order $\approx 10°/\text{h}$. For $\delta >$ Lat, $d\varphi/dt$ can be positive and negative. The minimum of $d\varphi/dt$ (= maximum of $|d\varphi/dt|$) is reached at $\phi = 0$ (see also Fig. 18). The maximum of $d\varphi/dt$ is also in the order $\approx 10°/\text{h}$.

The dynamical range of $d\varphi/dt$, defined as $D = |d\varphi/dt|_{\max}/|d\varphi/dt|_{\min}$ is plotted in the lower graph of Fig. 21 for $\delta <$ Lat. D is below 10 for $\delta \leq 15°$, and it rises steeply when δ approaches Lat. For $\delta >$ Lat D is infinite, because $|d\varphi/dt|_{\min}$ is equal to zero.

A final remark is in order: Throughout this report an implicit demand was that the source should stay in the center of the camera while it is being tracked. If this requirement is dropped, the extreme values of $|d\alpha/dt|$ and $|d\varphi/dt|$ can be reduced by letting the telescope point into a direction $(\theta,\, \varphi)$ with $\theta > \theta_{\text{source}}$ and $\varphi \approx \varphi_{\text{source}}$.

7.4 Alternative ways of moving the telescope

So far it has been implicitly assumed in this report that the orientations of the telescope are restricted to the region $0 < \theta < \theta_{\max}$. Actually, a telescope like MAGIC has a larger range of orientations: e.g. the telescope may be rotated, at fixed azimuthal angle φ, not only from a zenith angle $\theta (> 0)$ to $\theta = 0$ (mode **a**), but also beyond this value (mode **b**). The corresponding θ values will be given a minus sign. With MAGIC θ values down to $-80°$ or $-90°$ will be possible. In mode **a** the orientation of the telescope for observing a source at $(\theta,\, \varphi)$ would be also $(\theta,\, \varphi)$. In mode **b** the orientation of the telescope for observing the same source would be $(-\theta,\, \varphi\, +\, 180°)$.

A source may be observed entirely in mode **a** or entirely in mode **b**. When one wants to change the mode of observation during tracking of a source, one has to rotate the telescope around the horizontal axis from θ to $-\theta$ and around the vertical axis from φ to $\varphi + 180°$. Thus, the observation has to be interrupted while the re-orientation of the telescope is performed. Note that if no use is made of mode **b**, the observation may have to be interrupted because of limitations in the range of φ (see sectin 7.2). In this case, the telescope has to be rotated by 360° in φ before the observation can be continued .

Making full use of the two modes of observation, the minimum φ range necessary to observe all possible sources is 180°, say from φ_0 to $(\varphi_0 + 180°)$. When during observation of a source the boundary of this φ range is hit, the mode of observation has to be changed, requiring a re-orientation of the telescope from $(\theta,\, \varphi)$ to $(-\,\theta,\, \varphi + 180°)$.

A suitable choice of φ_0 is $\varphi_0 = 90°$ (east direction). In this case all sources with $\delta \lesssim 0°$ can be observed without interruption (see Fig. 19). Sources with $0 \lesssim \delta <$ Lat have to be observed in mode **a** most of the time, and in mode **b** part of the time (see Fig. 19). Sources with $\delta >$ Lat can be observed in mode **b** without interruption (see Fig. 19).

If one wants to observe all sources without interruption, the φ range within which the telescope can be moved has to be chosen large enough, in general greater than 360° (see section 7.2).

Table 1: Rotation speed and times for passing a fine- or low-resolution pixel for different values or regions of the declination.

declination of source	rotation speed ($\lvert d\alpha/dt \rvert$)	time for passing: fine-resolution pixel	time for passing: low-resolution pixel
$\delta \approx 90^\circ$	$\frac{360^\circ}{24\,\mathrm{h}} = \frac{0.25^\circ}{\mathrm{min}}$	21.8 min	30.0 min
$\lvert\delta - \mathrm{Lat}\rvert > 10^\circ$	$< \frac{1.33^\circ}{\mathrm{min}}$	$>$ 4.1 min	$>$ 5.6 min
$\lvert\delta - \mathrm{Lat}\rvert = 3^\circ$	$> \frac{2^\circ}{\mathrm{min}}$ for 30 min	$<$ 2.7 min	$<$ 3.8 min
	$\mathrm{max} = \frac{4.3^\circ}{\mathrm{min}}$	$>$ 1.3 min	$>$ 1.7 min
$\lvert\delta - \mathrm{Lat}\rvert = 1^\circ$	$> \frac{2^\circ}{\mathrm{min}}$ for 20 min	$<$ 2.7 min	$<$ 3.8 min
	$> \frac{5.5^\circ}{\mathrm{min}}$ for 10 min	$<$ 1.0 min	$<$ 1.4 min
	$\mathrm{max} = \frac{12.7^\circ}{\mathrm{min}}$	$>$ 0.43 min	$>$ 0.59 min

Lat = latitude of La Palma = 28.8°

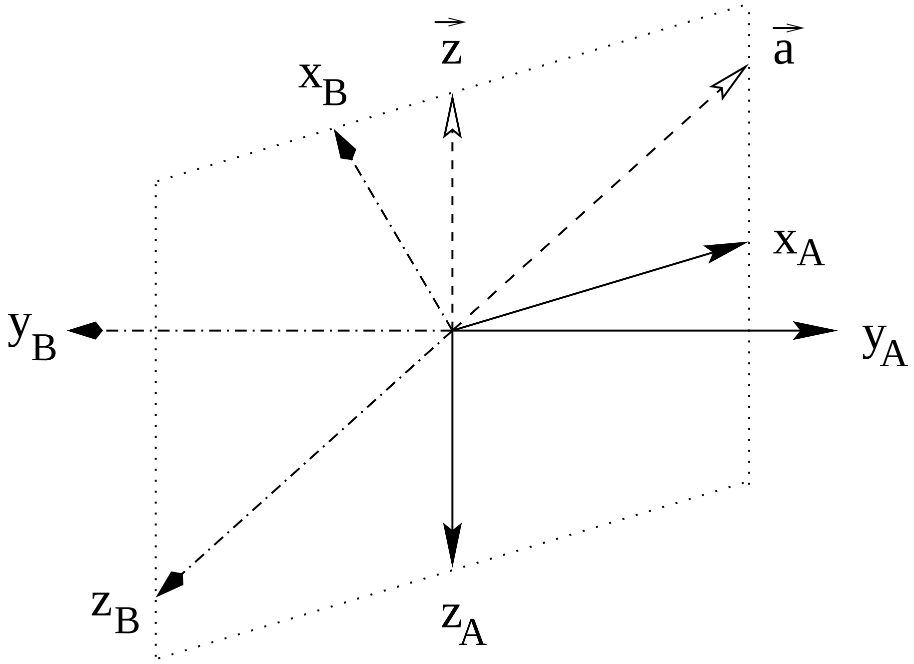

Figure 1: Directions of the axes ($x_{\rm A}$, $y_{\rm A}$, $z_{\rm A}$) and ($x_{\rm B}$, $y_{\rm B}$, $z_{\rm B}$) of the systems A and B respectively. The plane formed by the earth-rotation axis $\vec{a}$ and the zenith direction $\vec{z}$ contains also the directions $x_{\rm A}$, $z_{\rm A}$ and $x_{\rm B}$, $z_{\rm B}$. The directions $y_{\rm A}$ and $y_{\rm B}$ are perpendicular to this plane. The zenith direction $\vec{z}$ is opposite to $z_{\rm A}$, and $\vec{a}$ is opposite to $z_{\rm B}$.

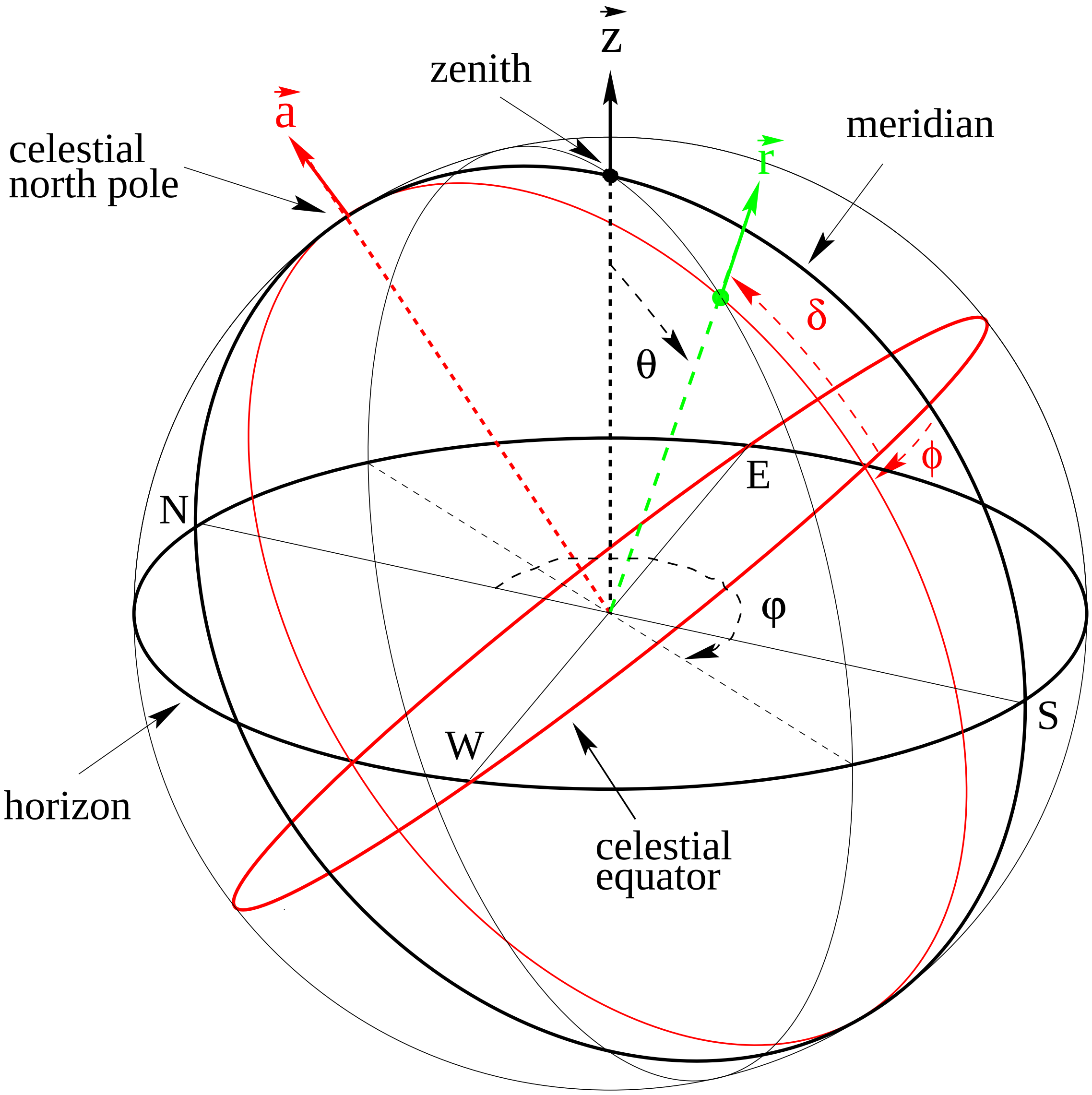

Figure 2: Definition of the zenith angle θ, the azimuthal angle φ, the declination δ and the hour angle ϕ. The vectors $\vec{a}$, $\vec{z}$ and $\vec{r}$ denote the earth-rotation axis, the zenith direction and the position of a point on the sky respectively.

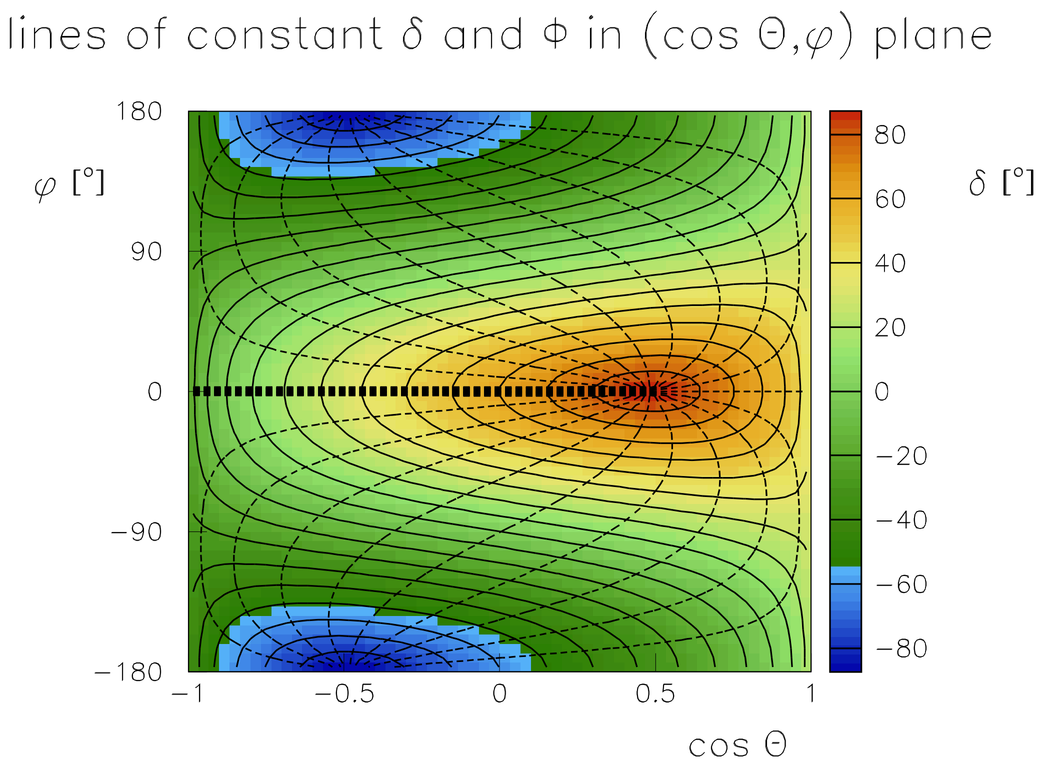

Figure 3: The lines of constant δ (solid lines) and constant ϕ (dashed lines) in the $(\cos\theta, \varphi)$ plane. The color scale indicates the respective value of δ. The point $(\cos\theta = -a_3, \varphi = 0)$ corresponds to the direction parallel $(\delta = 90°)$, the point $(\cos\theta = a_3, \varphi = 180°)$ to the direction antiparallel $(\delta = -90°)$ to the earth-rotation axis.

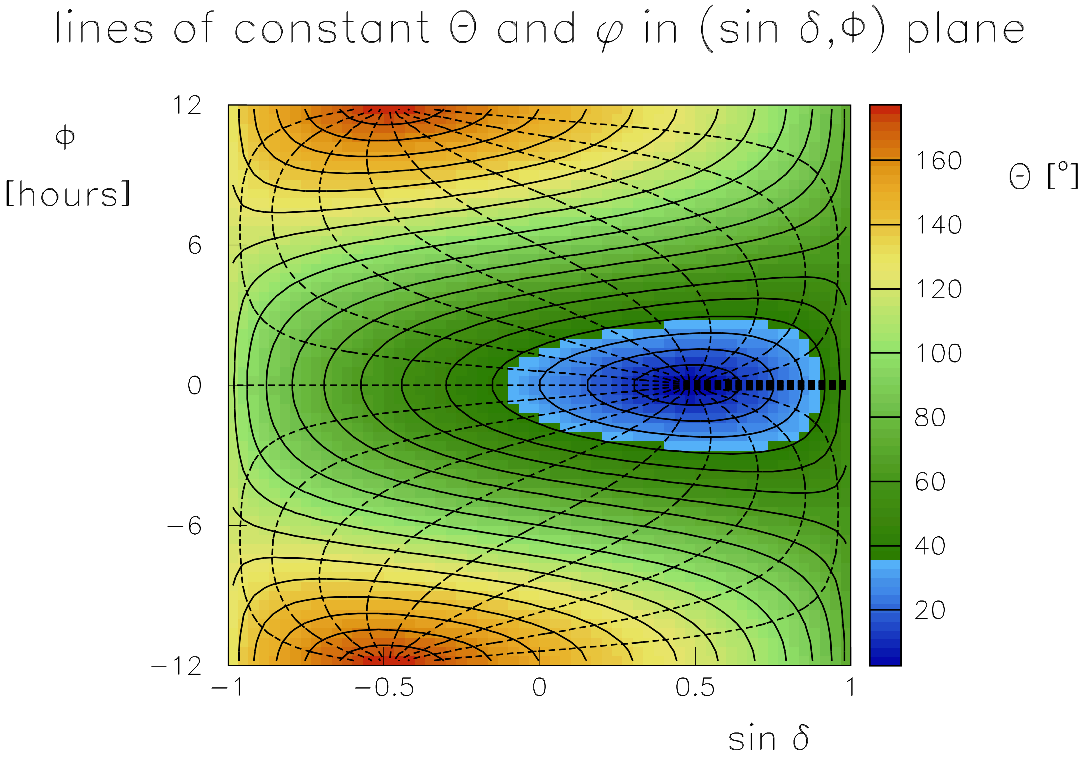

Figure 4: The lines of constant θ (solid lines) and constant φ (dashed lines) in the $(\sin\delta, \phi)$ plane. The color scale indicates the respective values of θ. The point $(\sin\delta = -a_3, \phi = 0)$ corresponds to the zenith $(\theta = 0)$, the point $(\sin\delta = a_3, \phi = 12\,\text{h})$ to the nadir $(\theta = 180°)$.

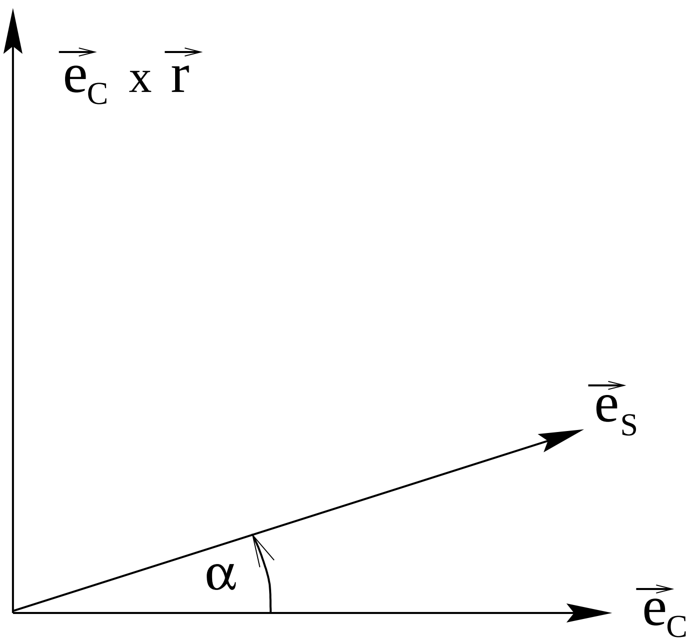

Figure 5: Definition of the rotation angle α of the sky image in the camera. $\vec{e}_{\rm c}$ and $\vec{e}_{\rm s}$ are reference directions in the camera and in a local sky region respectively. $\vec{r}$ denotes the direction in which the telescope is pointing. $\vec{e}_{\rm c}$ is defined as $(\vec{r}\times\vec{z})/|\vec{r}\times\vec{z}|$ where $\vec{z}$ is the zenith direction. $\vec{e}_{\rm s}$ is defined as $(\vec{r}\times\vec{a})/|\vec{r}\times\vec{a}|$ where $\vec{a}$ is parallel to the earth-rotation axis (pointing to the celestial north pole).

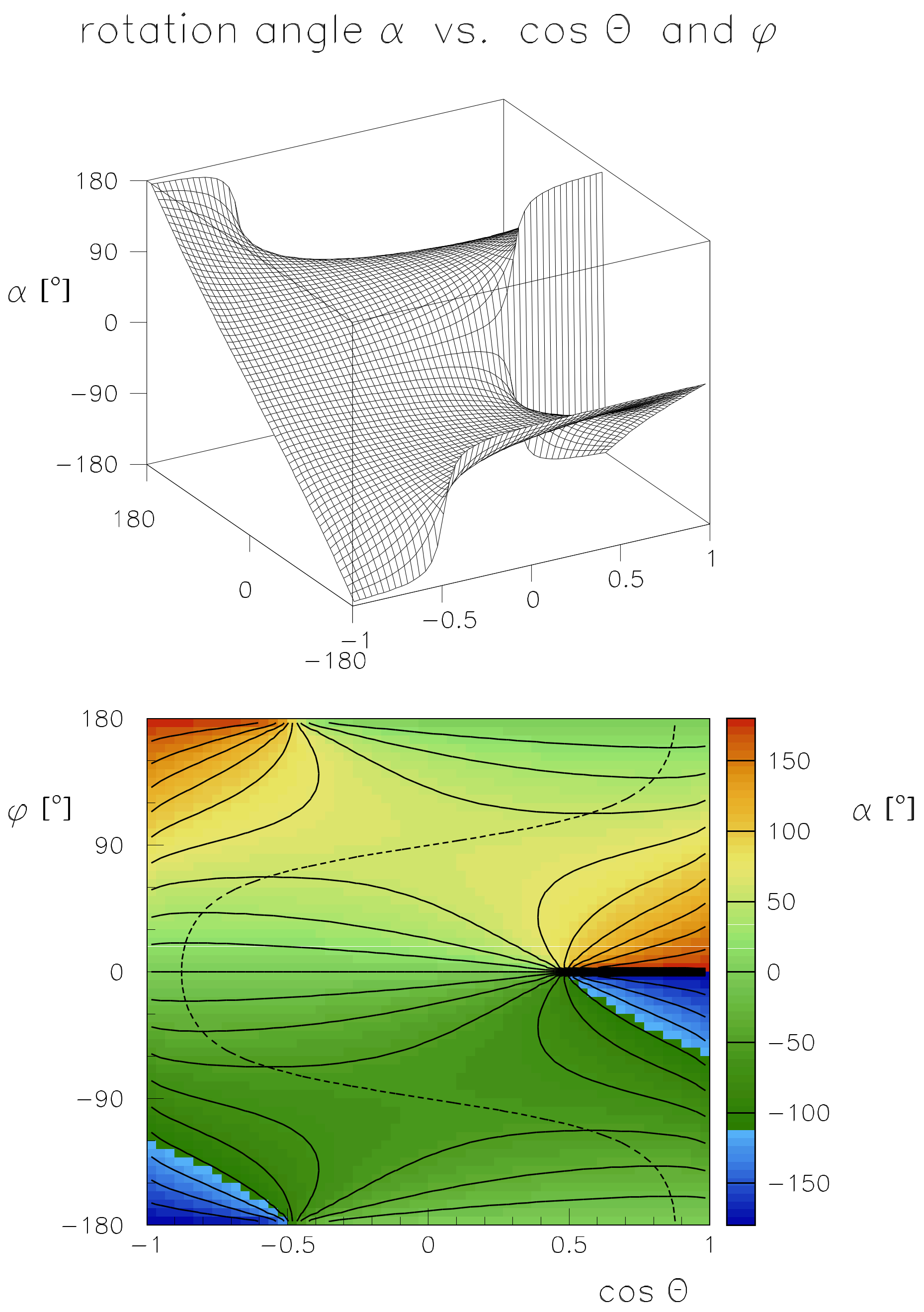

Figure 6: Rotation angle α as a funtion of $\cos\theta$ and φ (upper plot). In the lower plot the solid lines are the lines of constant α. The dashed line corresponds to $\delta = 0$.

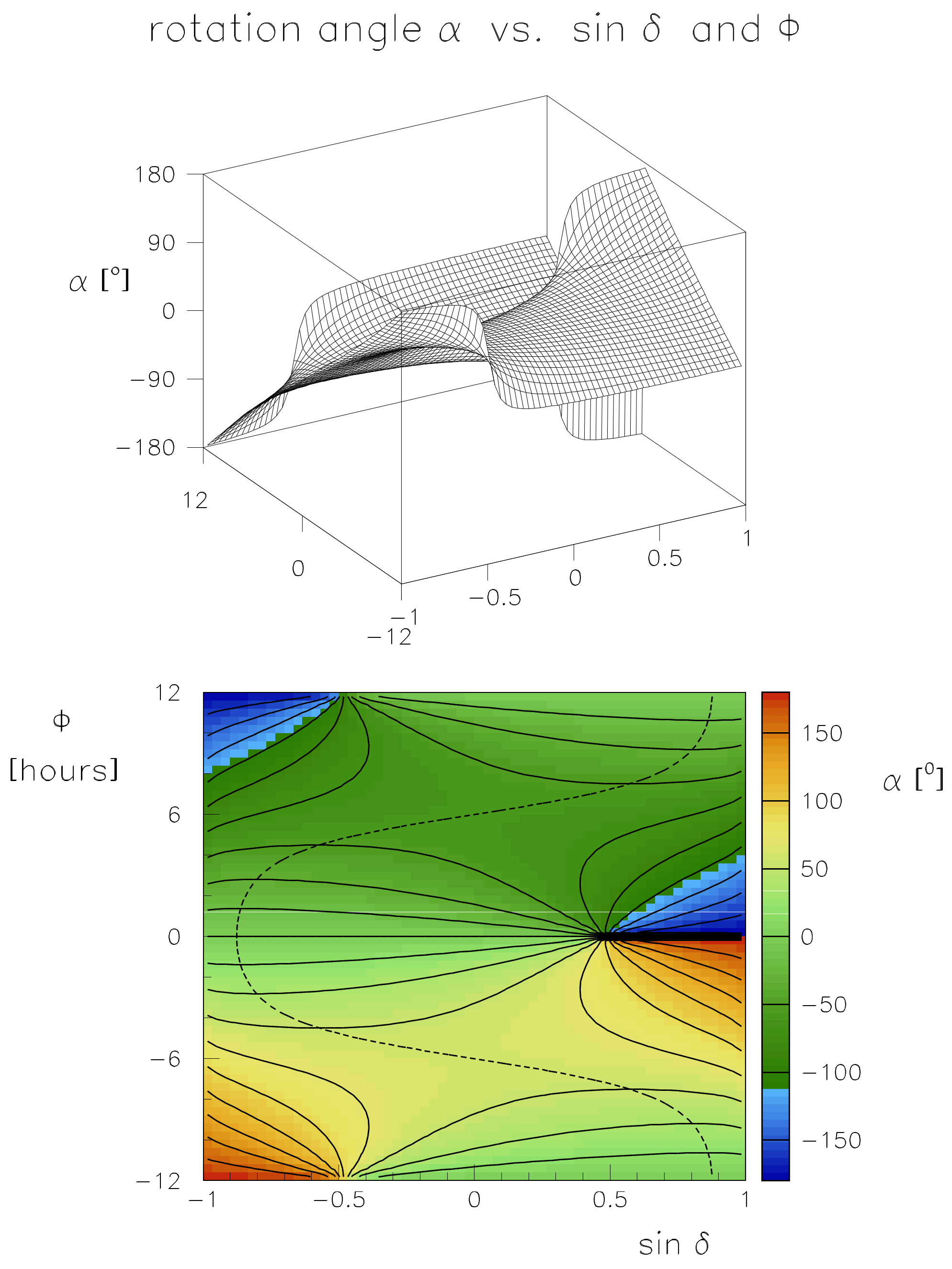

Figure 7: Rotation angle α as a funtion of $\sin\delta$ and ϕ (upper plot). In the lower plot the solid lines are the lines of constant α. The dashed line corresponds to $\theta = 90°$.

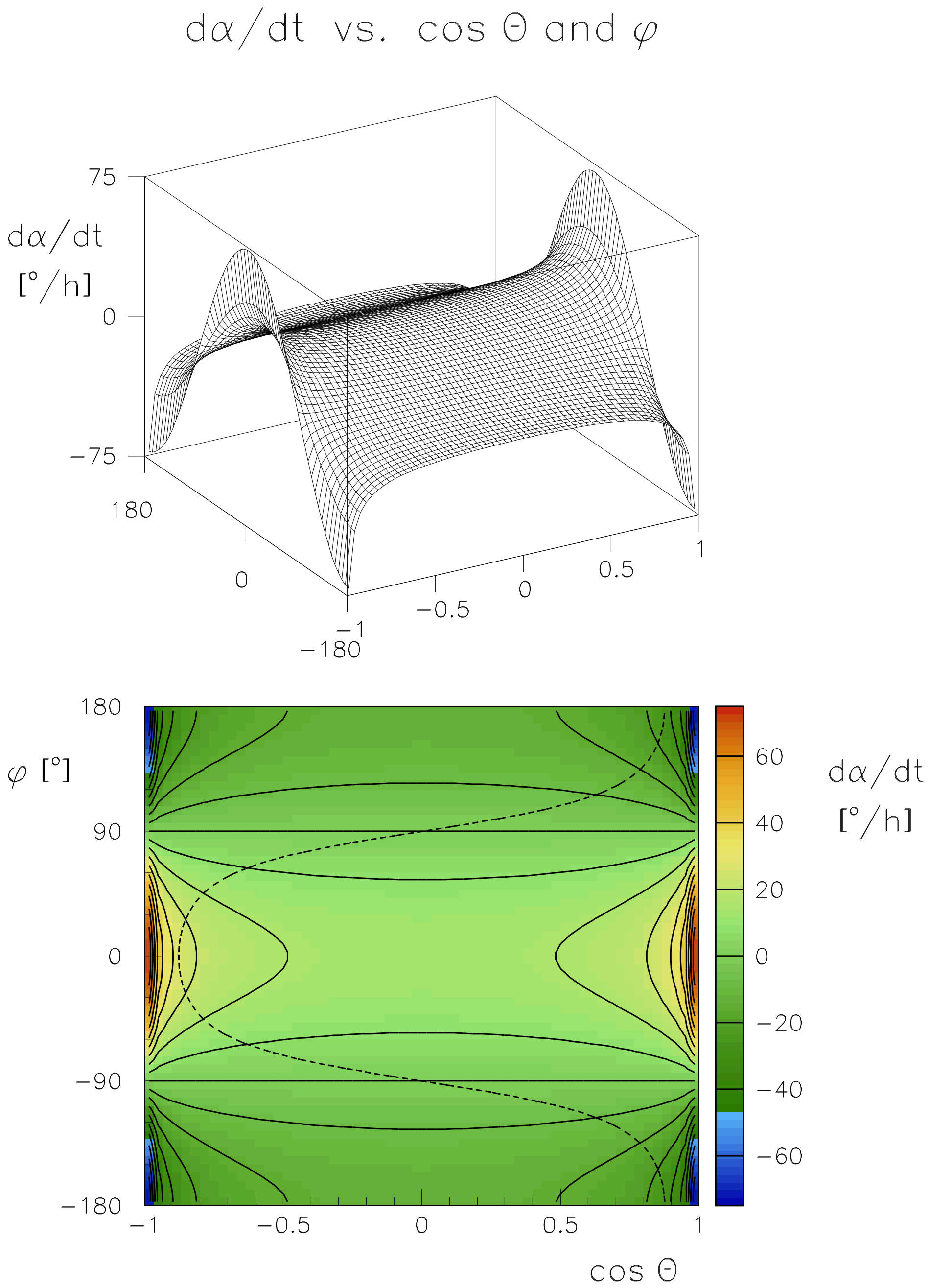

Figure 8: Rotation speed $d\alpha/dt$ as a function of $\cos\theta$ and φ (upper plot). In the lower plot the solid lines are the lines of constant $d\alpha/dt$. The dashed line corresopnds to $\delta = 0$.

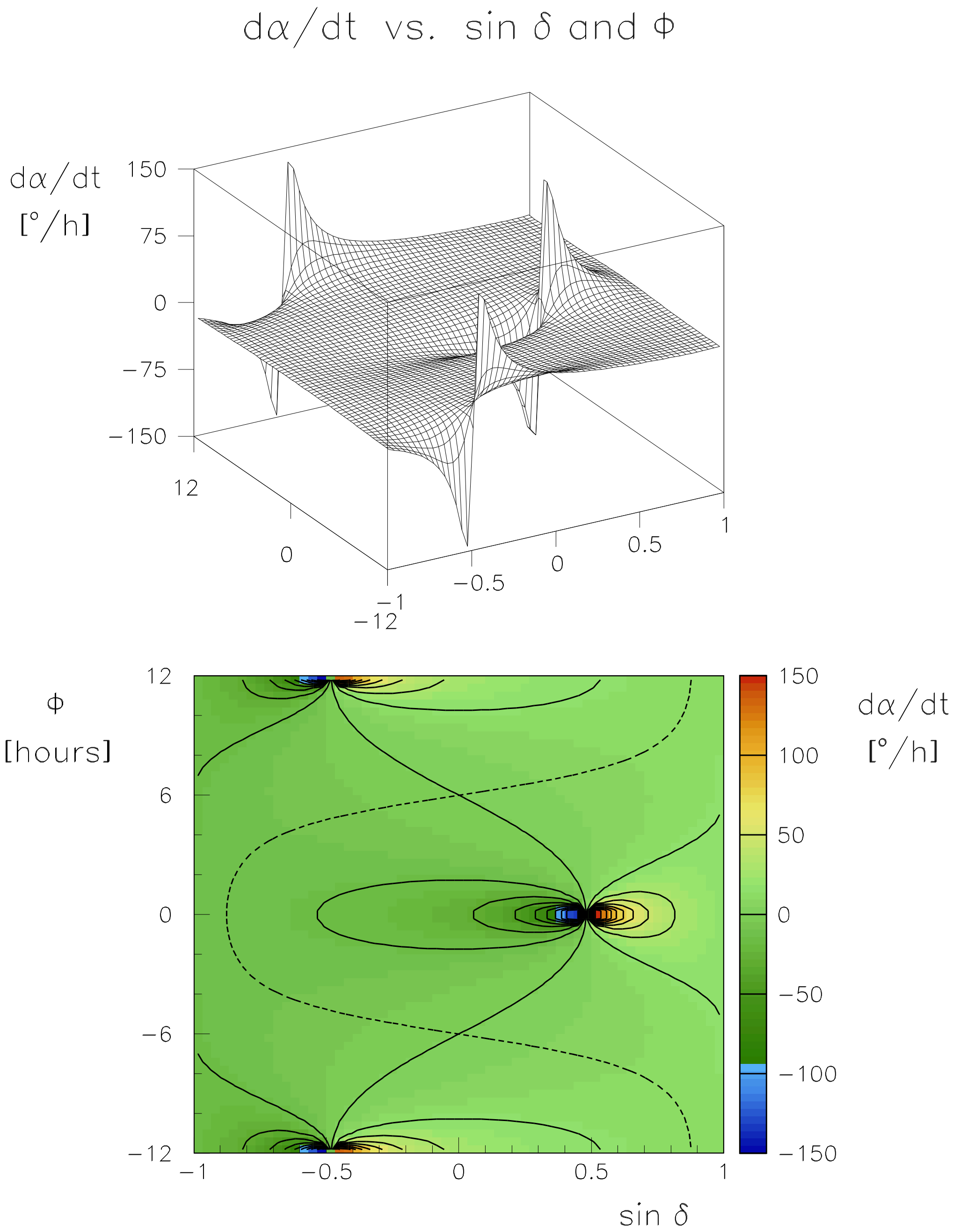

Figure 9: Rotation speed $d\alpha/dt$ as a function of $\sin\delta$ and ϕ (upper plot). In the lower plot the solid lines are the lines of constant $d\alpha/dt$. The dashed line corresponds to $\theta = 90°$.

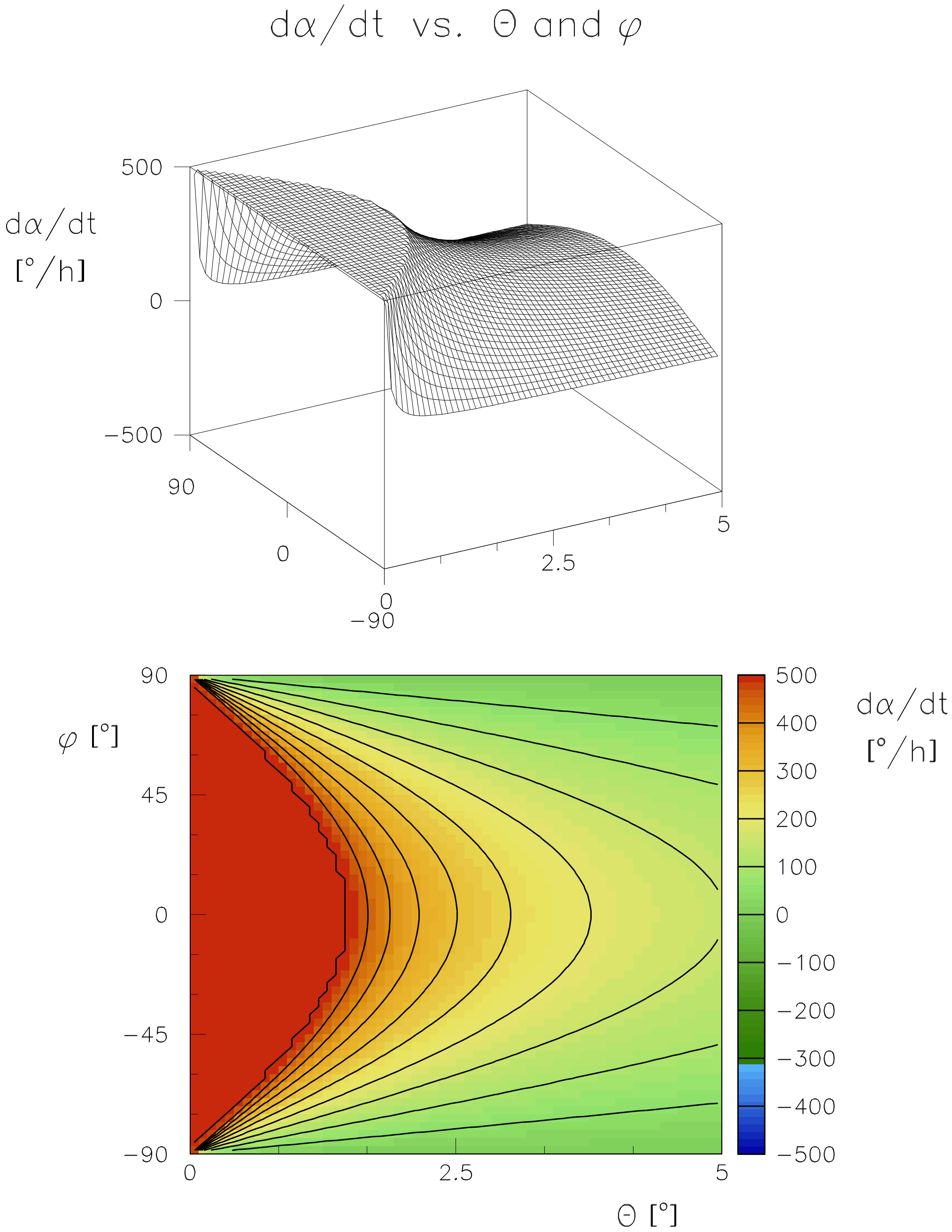

Figure 10: Rotation speed $d\alpha/dt$ as a function of θ and φ for a restricted region of θ and φ (upper plot). The lower plot shows the lines of constant $d\alpha/dt$. $d\alpha/dt$ is not drawn in the region where its absolute value is greater than 500°/h.

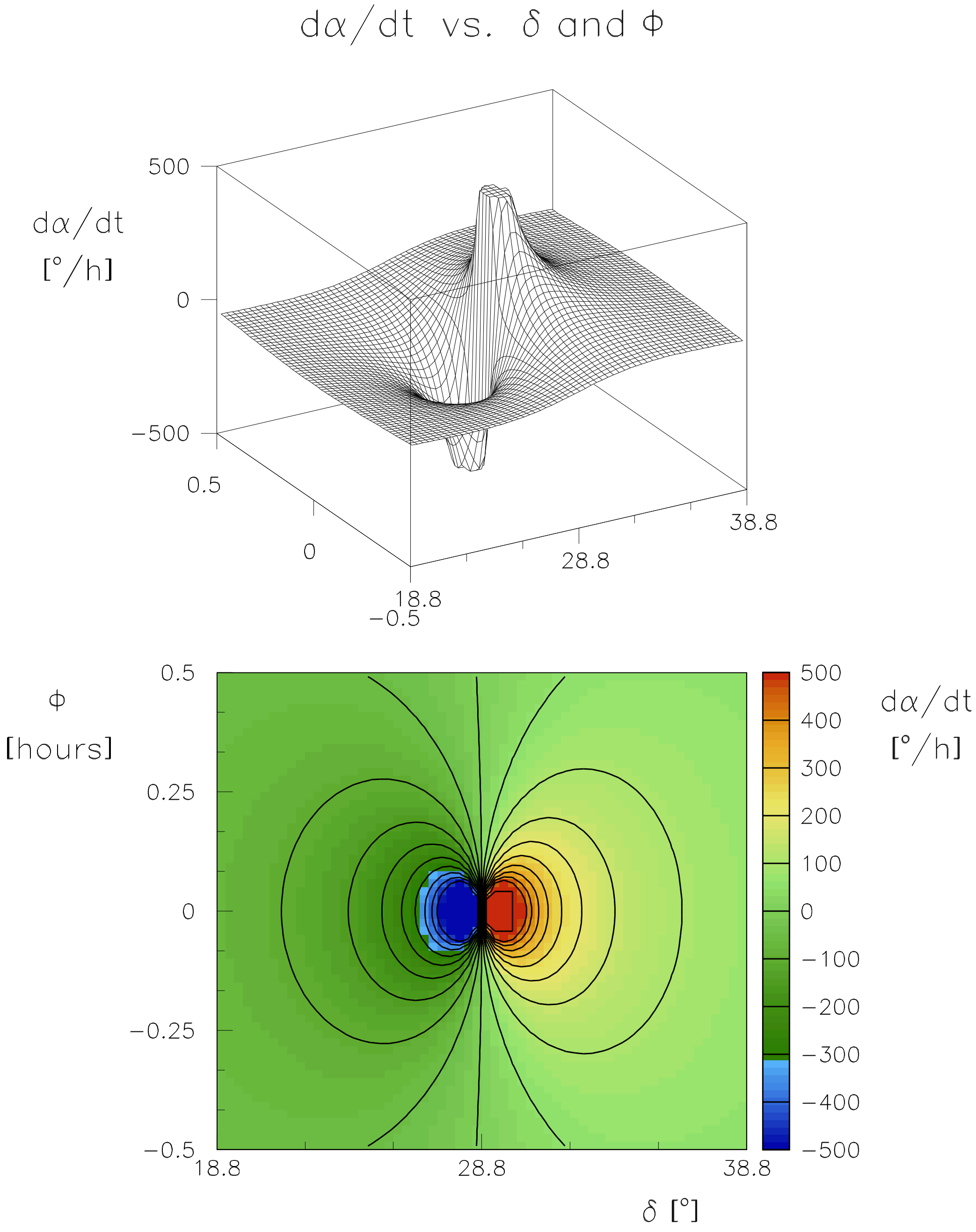

Figure 11: Rotation speed $d\alpha/dt$ as a function of δ and ϕ in a restricted region of δ and ϕ (upper plot). The lower plot shows the lines of constant $d\alpha/dt$. $d\alpha/dt$ is not drawn in the region where its absolute value is greater than 500°/h.

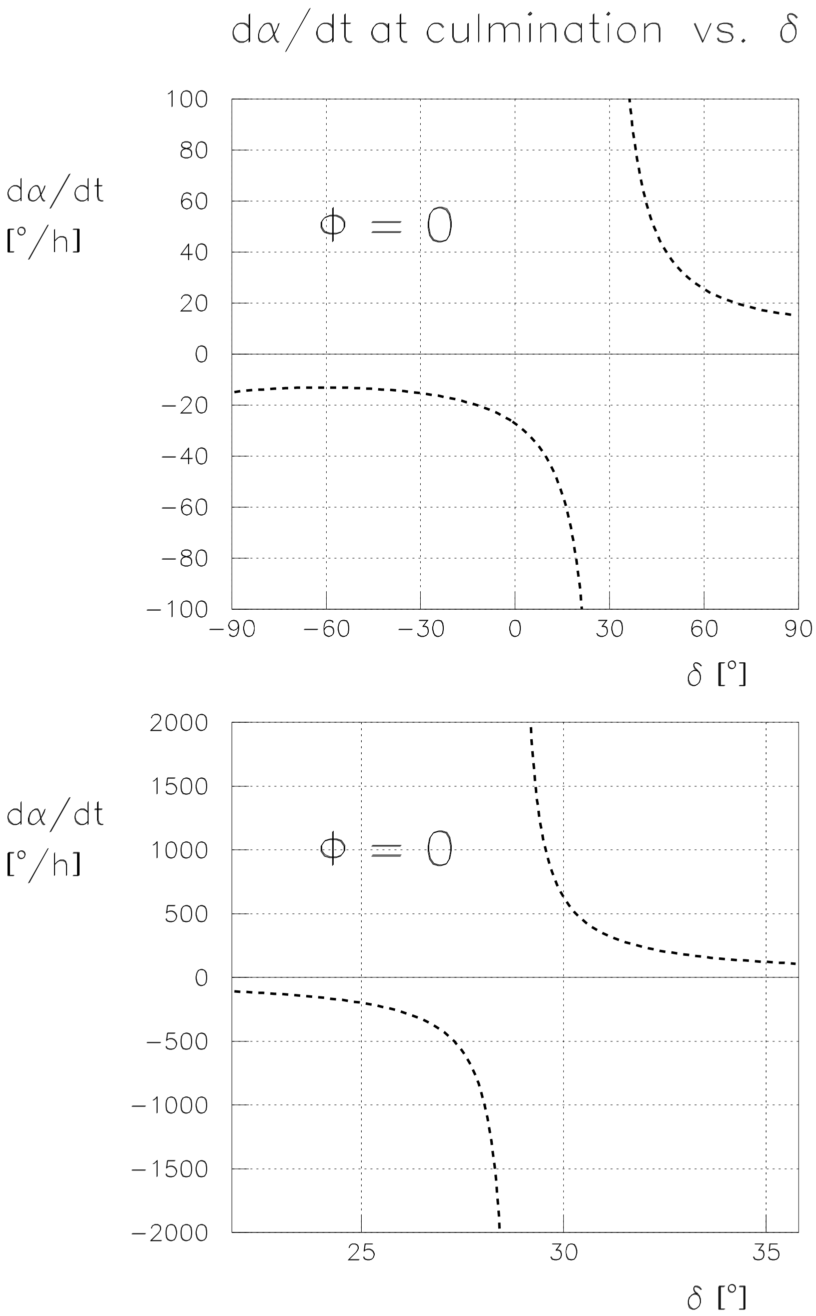

Figure 12: Rotation speed $d\alpha/dt$ for $\phi = 0$ as a function of δ, for the whole δ region (upper plot) and for a restricted region around $\delta = \text{Lat} = 28.8^\circ$ (lower plot).

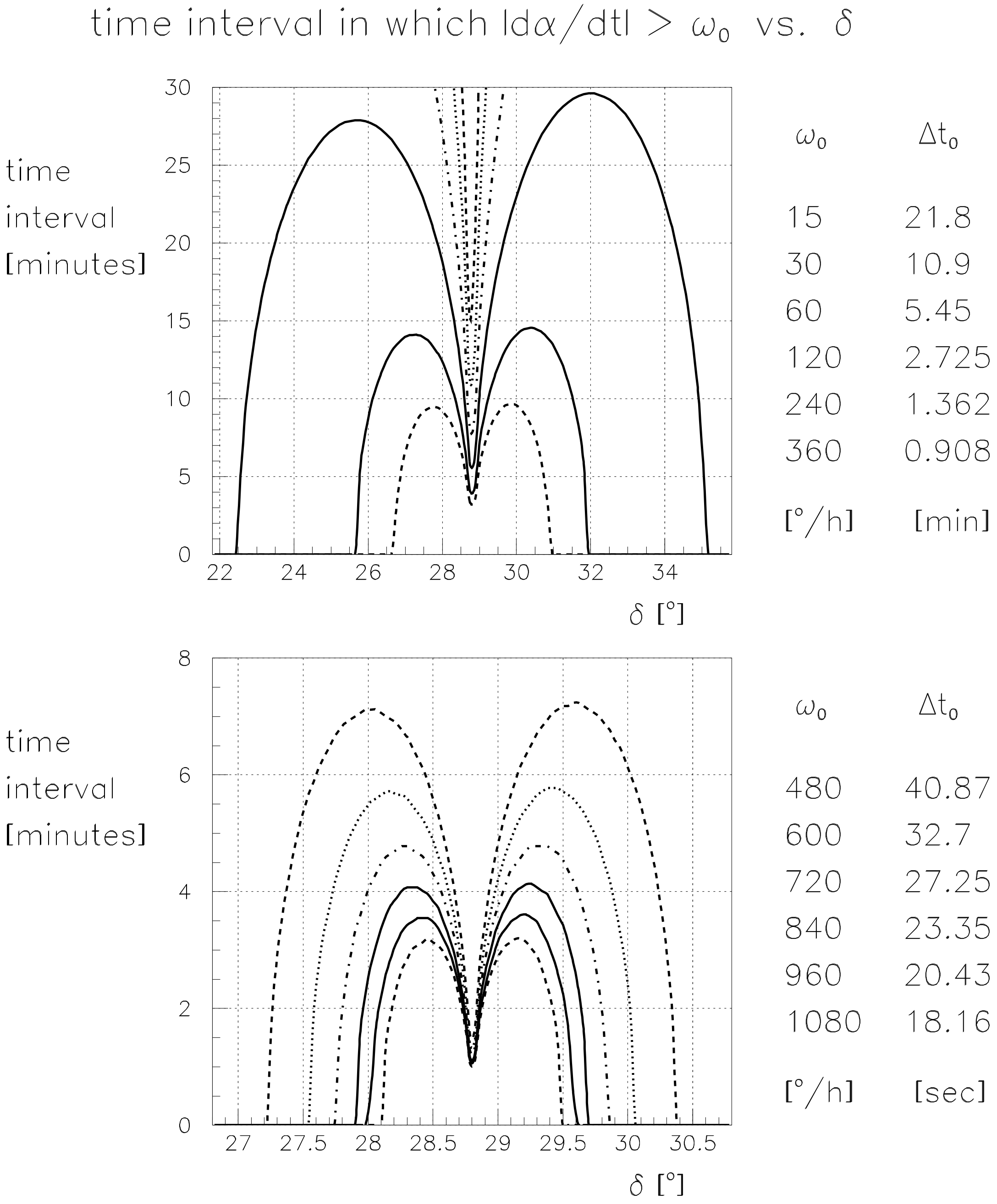

Figure 13: Length of the time interval in which $|d\alpha/dt|$ is greater than ω_0, plotted as a function of δ for different values of ω_0. Within these time intervals a fine-resolution pixel is passed in a time less than Δt_0. The order of the ω_0 and Δt_0 values corresponds to the order of the curves in the Figures: the most upper curve is for the most upper values of ω_0 and Δt_0, etc.

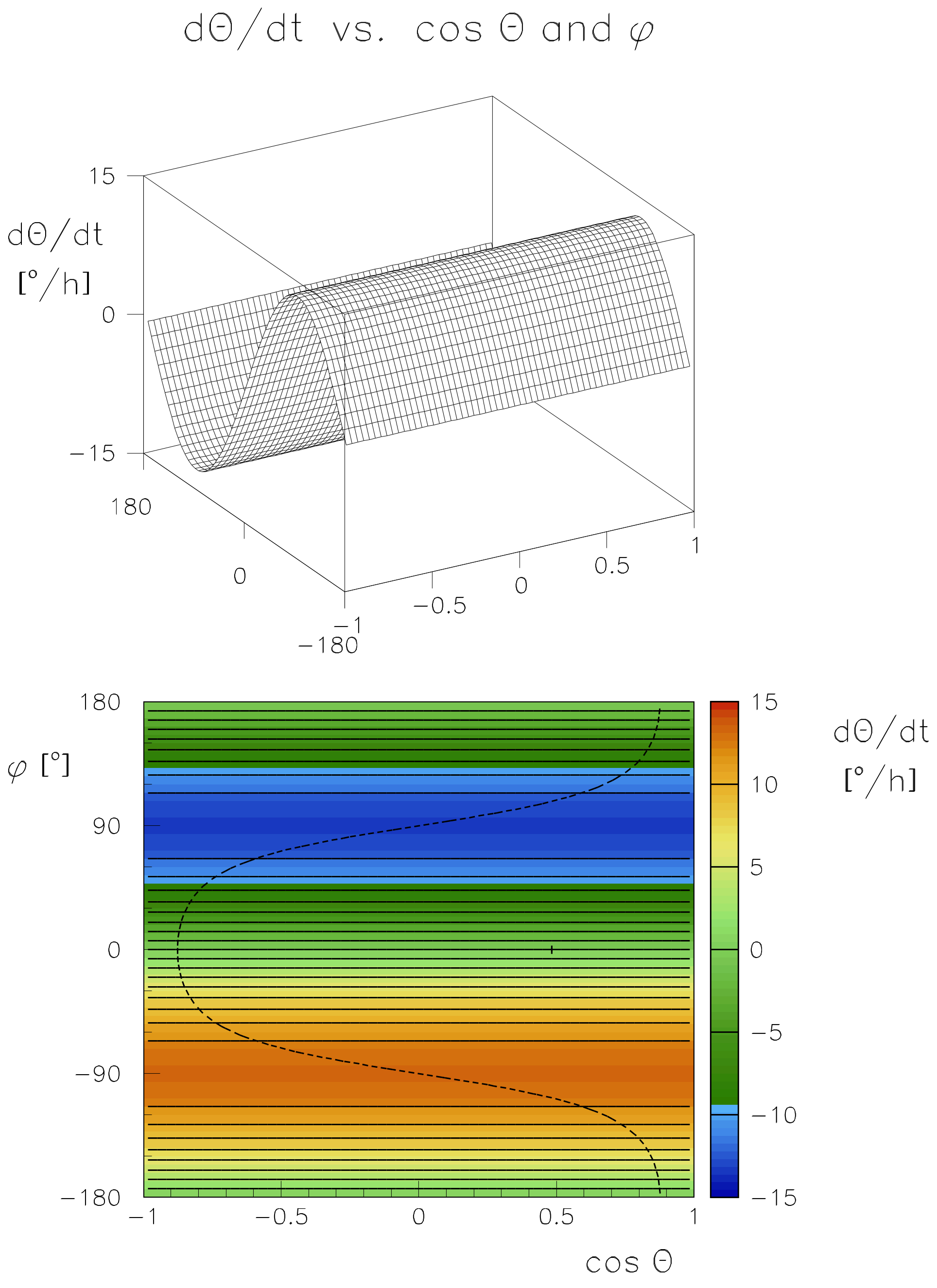

Figure 14: $d\theta/dt$ as a function of $\cos\theta$ and φ (upper plot). In the lower plot the solid lines are the lines of constant $d\theta/dt$. The dashed line corresponds to $\delta = 0$.

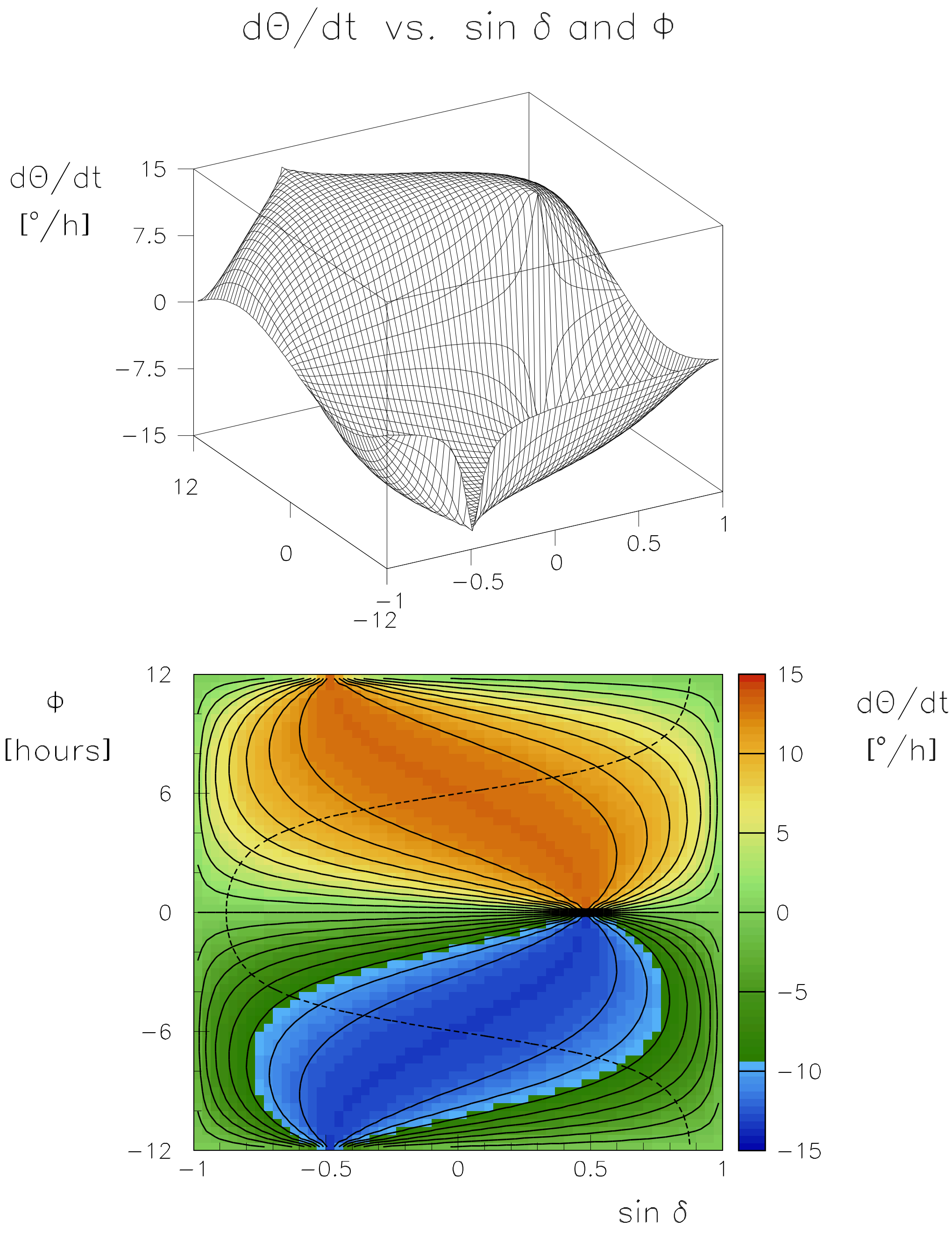

Figure 15: $d\theta/dt$ as a function of $\sin\delta$ and ϕ (upper plot). The lower plot shows the lines of constant $d\theta/dt$. The dashed line corresponds to $\theta = 90°$.

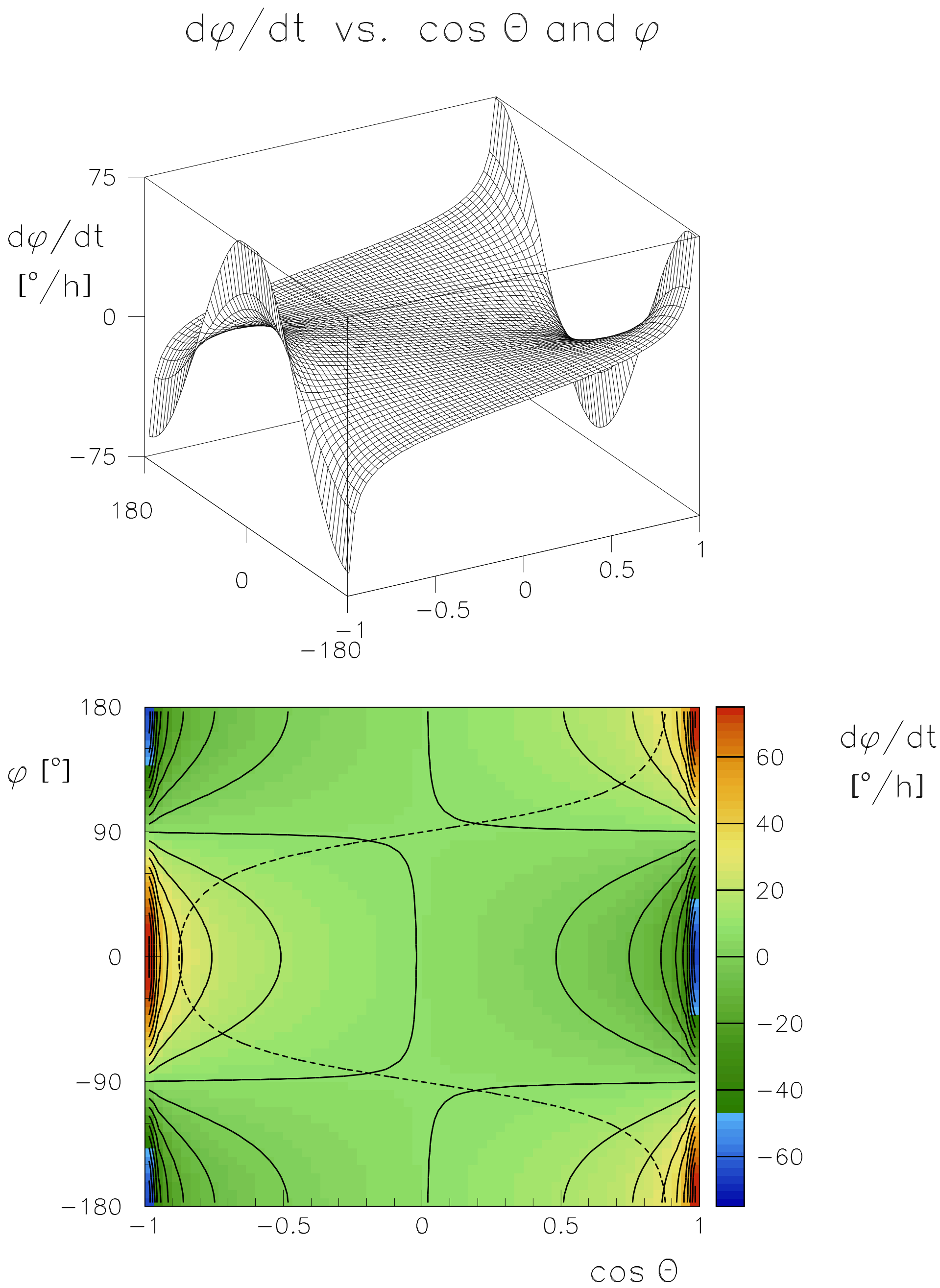

Figure 16: $d\varphi/dt$ as a function of $\cos\theta$ and φ (upper plot). In the lower plot the solid lines are the lines of constant $d\varphi/dt$. The dashed line corresponds to $\delta = 0$.

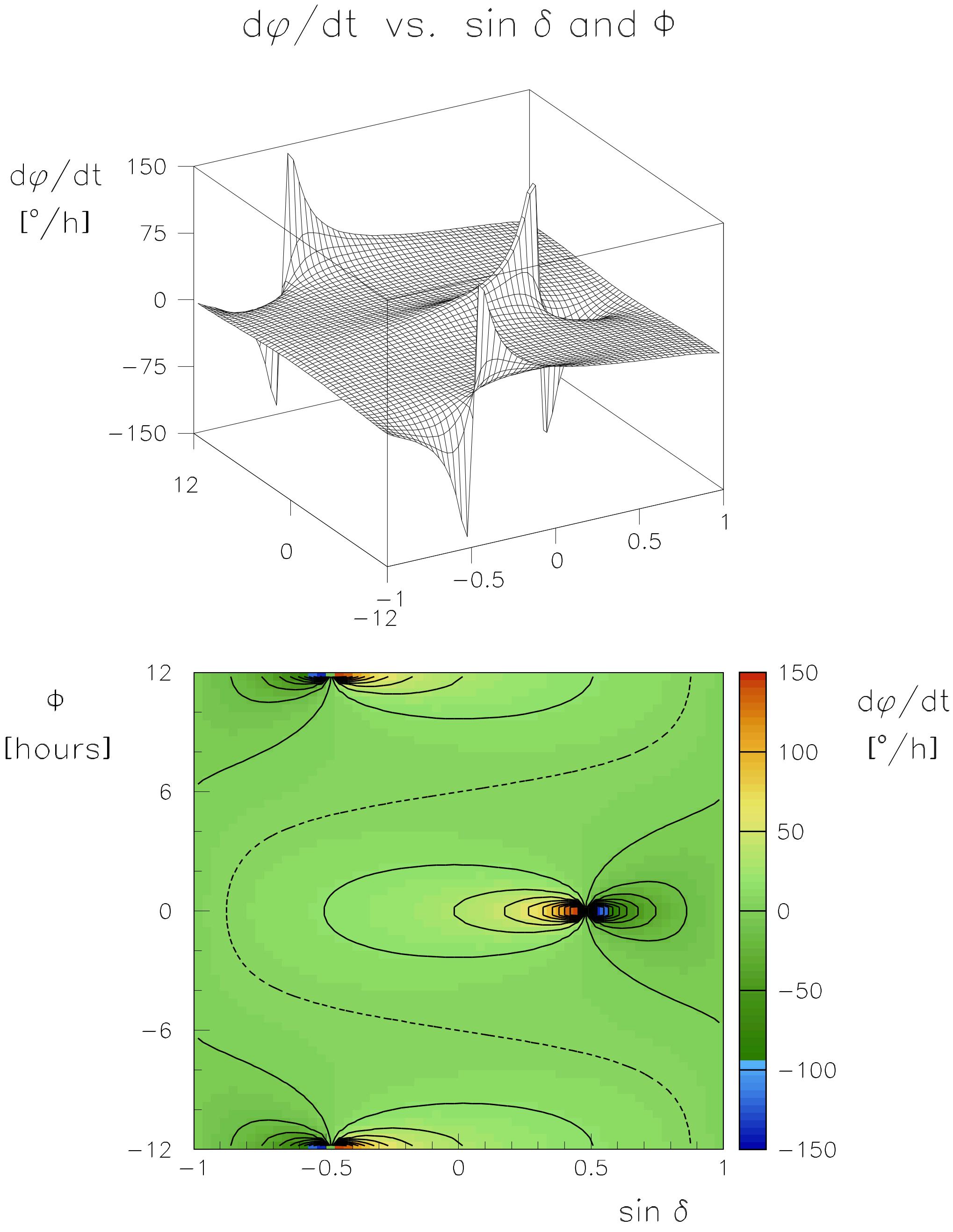

Figure 17: $d\varphi/dt$ as a function of $\sin\delta$ and ϕ (upper plot). The lower plot shows the lines of constant $d\varphi/dt$. The dashed line corresponds to $\theta = 90°$.

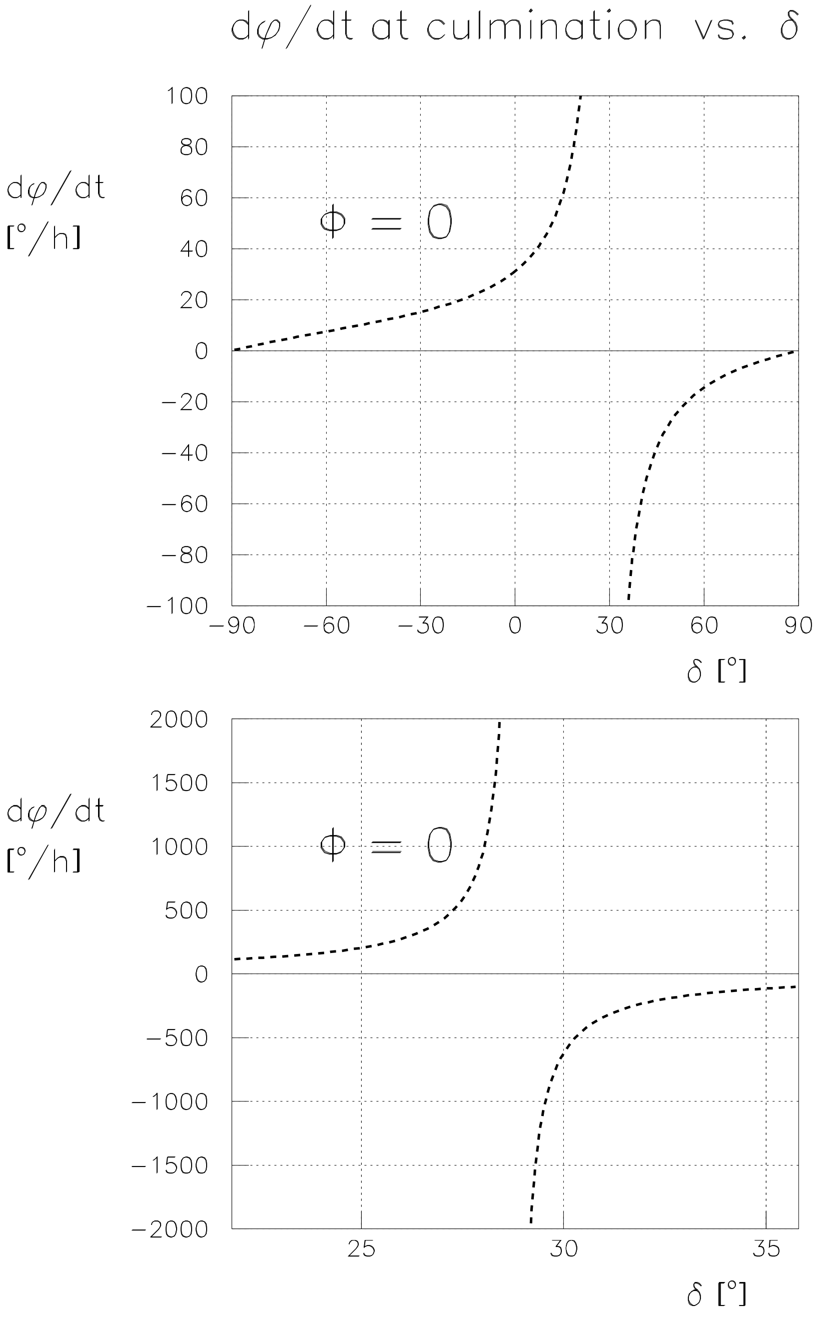

Figure 18: $d\varphi/dt$ for $\phi = 0$ as a function of δ, for the whole δ region (upper plot) and for a restricted region around $\delta = \mathrm{Lat} = 28.8°$ (lower plot).

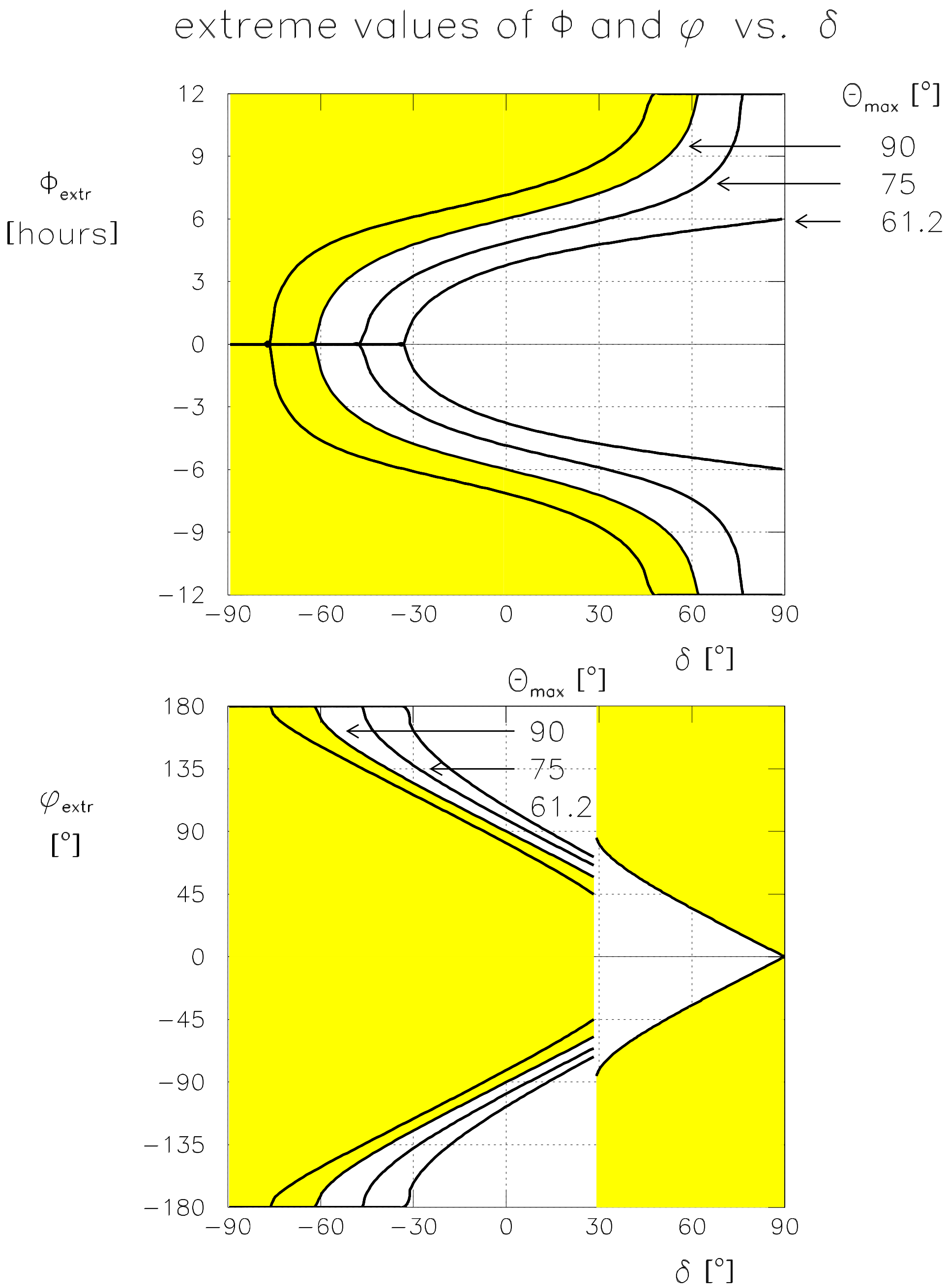

Figure 19: Upper plot: Extreme values of the hour angle ϕ as a function of δ, for $\theta_{\rm max} = 105^\circ, 90^\circ, 75^\circ$ and 61.2°. For $\theta_{\rm max} = 90^\circ$ the region which is not accessible during observation is shown shaded.
Lower plot: Extreme values of the azimuthal angle φ as a funtion of δ, for $\theta_{\rm max} = 105^\circ, 90^\circ, 75^\circ$ and 61.2°. For $\theta_{\rm max} = 90^\circ$ the region which is not accessible during observation is drawn shaded.

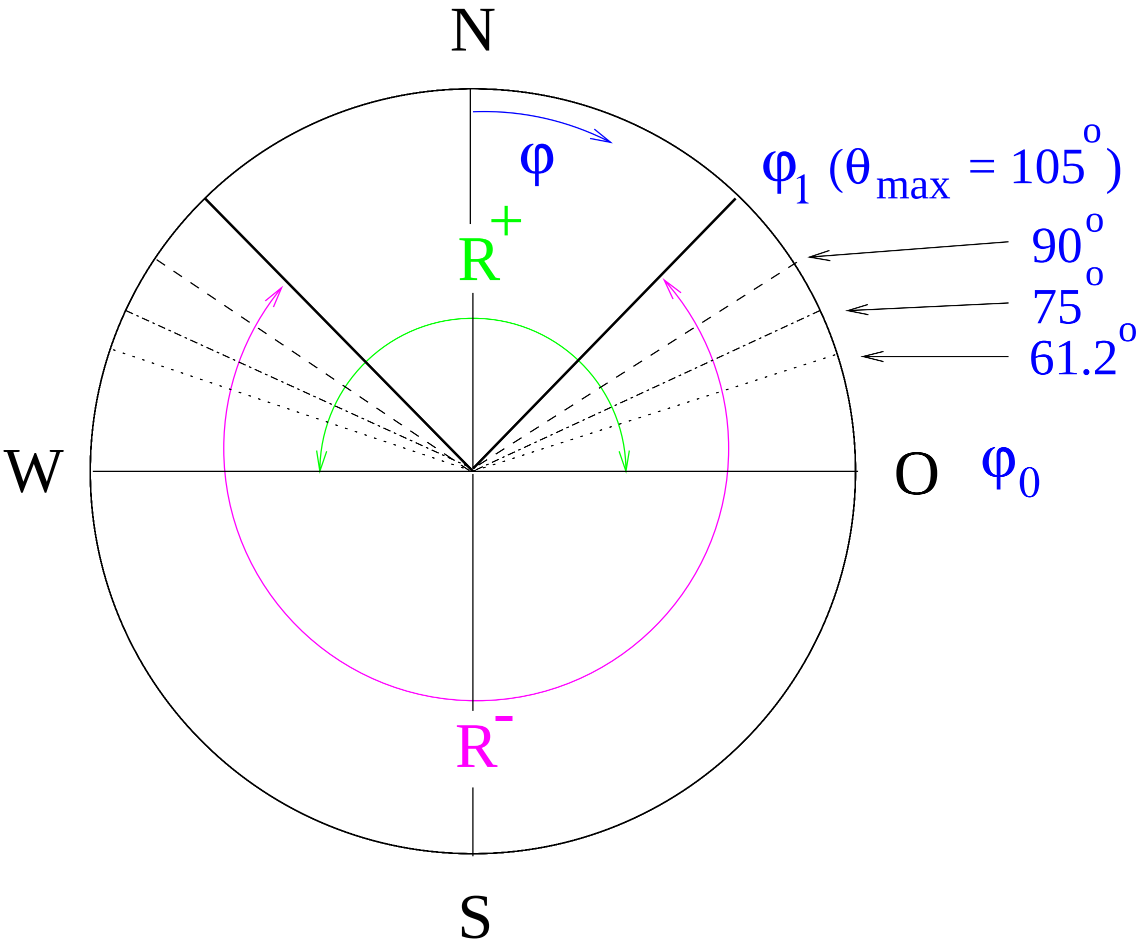

Figure 20: Ranges of φ covered by a source with δ slightly above Lat (R^+) and by a source with δ slightly below Lat (R^-) under the condition $\theta < \theta_{\rm max} = 105°$. The change of R^- with $\theta_{\rm max}$ is indicated.

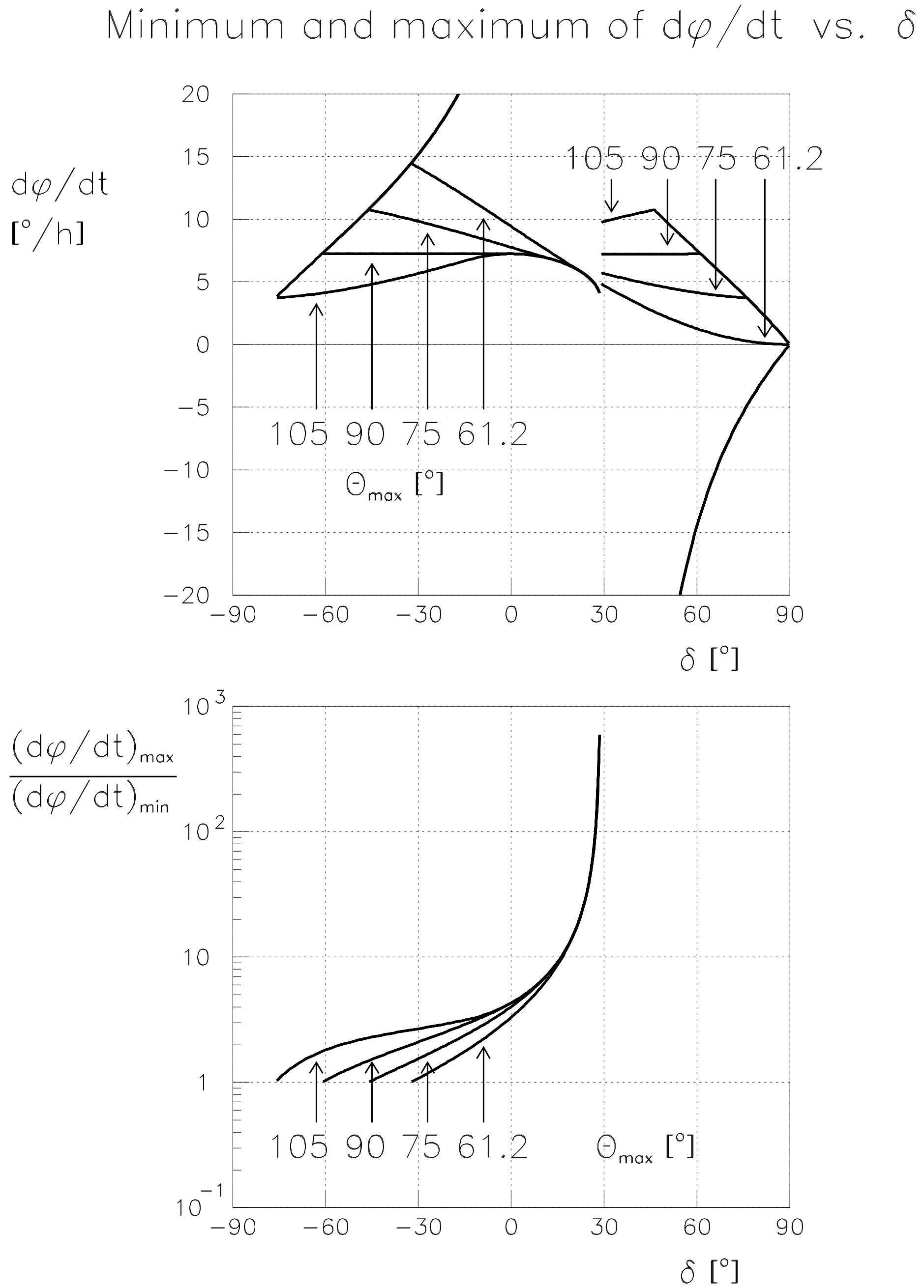

Figure 21: Upper plot: Minimum and maximum values of $d\varphi/dt$ as a function of δ, for $\theta_{\max} = 105°, 90°, 75°$ and $61.2°$. By comparing with Fig. 18 one can see that the maximum of $|d\varphi/dt|$ is reached at $\phi = 0$, i.e. when the source is culminating.
Lower plot: The ratio $(d\varphi/dt)_{\max}/(d\varphi/dt)_{\min}$ as a function of δ, for $\theta_{\max} = 105°, 90°, 75°$ and $61.2°$. Note that for $\delta >$ Lat $d\varphi/dt$ can be positive and negative, implying an infinite dynamical range.